

University of Montana

ScholarWorks at University of Montana

Graduate Student Theses, Dissertations, &
Professional Papers

Graduate School

2022

Development of regional landslide susceptibility models: a first step towards model transferability

Gina M. Belair

University of Montana, Missoula

Follow this and additional works at: <https://scholarworks.umt.edu/etd>



Part of the [Applied Statistics Commons](#), [Geomorphology Commons](#), and the [Statistical Models Commons](#)

Let us know how access to this document benefits you.

Recommended Citation

Belair, Gina M., "Development of regional landslide susceptibility models: a first step towards model transferability" (2022). *Graduate Student Theses, Dissertations, & Professional Papers*. 11870.
<https://scholarworks.umt.edu/etd/11870>

This Thesis is brought to you for free and open access by the Graduate School at ScholarWorks at University of Montana. It has been accepted for inclusion in Graduate Student Theses, Dissertations, & Professional Papers by an authorized administrator of ScholarWorks at University of Montana. For more information, please contact scholarworks@mso.umt.edu.

DEVELOPMENT OF REGIONAL LANDSLIDE SUSCEPTIBILITY MODELS:
A FIRST STEP TOWARDS MODEL TRANSFERABILITY

By

GINA MARIE BELAIR

B.A. Physics, University of California, Berkeley, California, 2015
B.A. Geophysics, University of California, Berkeley, California, 2015

Thesis

presented in partial fulfillment of the requirements
for the degree of

Master of Science
in Geosciences

The University of Montana
Missoula, MT

May 2022

Approved by:

Scott Whittenburg, Dean of The Graduate School
Graduate School

Marc Hendrix, Chair
Department of Geosciences

Rebecca Bendick, Committee Chair
Department of Geosciences

Andrew Wilcox, Committee Member
Department of Geosciences

Kevin McManigal, Committee Member
Department of Forest Management

TABLE OF CONTENTS

Abstract.....	iii
Chapter 1: Project Introduction.....	1
1 Research Motivations.....	1
2 Thesis Objectives.....	1
3 Research Methodology.....	2
4 Concluding Remarks.....	2
5 References.....	2
Chapter 2: Development of regional landslide susceptibility models: a first step towards model transferability.....	4
1 Introduction.....	4
2 Methods.....	7
3 Results.....	15
4 Discussion.....	22
5 References.....	25
6 Supplementary Information.....	31
Appendix A. Source Code.....	46

LIST OF FIGURES

1 Overview of methodological approach used in study.....	7
2 Study regions.....	12
3 Overview of workflows for susceptibility relationship development.....	14
4 Select ROC curves.....	18
5 Plot of logistic regression diagnostic statistics.....	18
6 Susceptibility and landslide occurrence map.....	20

LIST OF TABLES

1 Summary of study regions.....	13
2 Cutoff dependent diagnostic statistics.....	15
3 Regions with significant factors.....	16
4 Diagnostic statistics for single regions.....	17
5 Diagnostic statistics for single-region cross-validation.....	21
6 Diagnostic statistics for multi-region cross-validation.....	21

Development of regional landslide susceptibility models: a first step towards model transferability

Committee Chair: Rebecca Bendick

Committee Members: Andrew Wilcox, Kevin McManigal

Landslides are a globally pervasive problem with the potential to cause significant fatalities and economic losses. Although landslides are widespread, many at-risk regions may not have the high-quality data or resources used in most landslide susceptibility analyses. This study aims to develop regional susceptibility relationships that are versatile and use publicly available data and open-sourced software. Logistic Regression and Frequency Ratio susceptibility relationships were developed in 23 regions in Washington, Utah, North Carolina, and Kentucky, with a region referring to a unique area and data combination. Regions were diverse in their geology, morphology, climate, and nature and quality of their landslide data. The transferability of select models to regions uninvolved in model development was also tested. The transferred models were trained using data from a single region (single-region cross-validation) or a combination of regions (multi-region cross-validation). Potential landslide contributing factors were all derived from a globally available digital surface model while landslide inventories were publicly available from state geological surveys. The contributing factors considered were elevation, slope, aspect, planform curvature, profile curvature, and topographic position index. Models developed using high-quality landslide data delineating scarps, flanks, and individual slope movements performed very well (AUC 0.764 - 0.895; AUC = area under relative operating characteristics curve). Models developed using landslide data dominated by deposits performed less well, but at or near an acceptable level (AUC 0.67 – 0.81). Models developed using older, lower quality landslide data did not perform at an acceptable level (AUC 0.63 – 0.64). The results of testing model transferability had acceptable results for some but not all regions (AUC 0.563 - 0.844). This study is a promising first step in developing generalized landslide susceptibility relationships that can be used in areas that share similar regional scale attributes.

Chapter 1: Project Introduction

1 Research Motivations

The damage caused by landslides can be catastrophic, both socially and economically. To minimize the damage incurred, landslide susceptibility assessments are conducted to determine areas of potential mass movements. Landslide susceptibility models are most commonly generated from physics-based slope failure models, or from heuristic or statistical analysis of past landslide occurrence (Aleotti & Chowdhury, 1999; Guzzetti et al., 1999; Reichenbach et al., 2018a; van Westen et al., 2006; and references therein). The majority of advancements in landslide susceptibility research are implemented in a narrow set of circumstances, require high-resolution data, and their transferability to other regions is largely untested. Many communities with high landslide risk do not have resources to employ these methods. This study aims to develop more general regional landslide susceptibility models, a necessary first-step in developing models that can be transferred to unstudied regions.

There are a multitude of different qualitative and quantitative methods used to assess landslide susceptibility, with the preferred method depending on the level of expertise of the practitioner and the available resources. The majority of assessment methods are dependent on landslide inventories, the compilation of which are often small-scale and site specific. Landslide inventories are created by visual identification from aerial photographs (e.g., Ayalew & Yamagishi, 2005), satellite images (e.g., Feizizadeh & Blaschke, 2014), stereoscopic images (e.g., Fiorucci et al., 2019), and LiDAR images (e.g., Van Den Eeckhaut et al., 2007). There are also semi-automatic detection methods based on surface roughness (e.g., Berti et al., 2013). Many countries do not have a national database of events, and if they do they contain inconsistent and incomplete data. In the United States, a national database was only released by the USGS in October 2019 (Jones et al., 2019). The lack of complete, high-quality landslide inventories supports the need to develop susceptibility models that can be applied to regions without inventories.

Due to the diversity of climates, geology, land development, and landslide mechanisms it is unlikely there is a single statistical relationship that can accurately predict landslide occurrence everywhere. Yet multiple studies provide evidence that under certain circumstances susceptibility models can be transferred to regions not used in model training (e.g., Kritikos et al., 2015; Lee, 2005; Von Ruetten et al., 2011). It is possible this process can be expanded to other generic study regions. Although this has the potential to oversimplify a very complicated system, it can be used as a first-order approach in regions that lack data and resources.

2 Thesis Objectives

The primary goals of this study were to: 1) develop a landslide susceptibility method that can be implemented in diverse regions, 2) ensure the method is versatile and uses publicly available data and open-source software, 3) move towards susceptibility relationships that can be applied to unstudied regions without landslide inventories.

3 Research Methodology

Statistical landslide susceptibility models were developed using logistic regression and frequency ratio methods. The landslide contributing factors (i.e., independent variables) were “simple” morphological variables derived from a 30 m globally available digital surface model. Landslide occurrence data (i.e., dependent variable) were from publicly available landslide inventories from state geological surveys. Models were developed and tested in all regions, while select models were applied in regions uninvolved in training. Four diagnostic statistics were used to assess the performance of the models.

4 Concluding Remarks

This study is promising progress towards the creation of susceptibility models that can be applied to regions uninvolved in model training. The developed method is easy to implement, interpret, uses publicly available data, and open-source software. The method works as expected, with higher quality landslide data providing better results than lower quality data. It is also expected that landslide data that distinguishes by process domain (e.g., scarps and flanks versus deposits) will create better performing models, since each process domain provides unique information about landslide occurrence.

5 References

- Aleotti, P., & Chowdhury, R. (1999). Landslide hazard assessment: Summary review and new perspectives. *Bulletin of Engineering Geology and the Environment*, 58(1), 21–44. <https://doi.org/10.1007/s100640050066>
- Ayalew, L., & Yamagishi, H. (2005). The application of GIS-based logistic regression for landslide susceptibility mapping in the Kakuda-Yahiko Mountains, Central Japan. *Geomorphology*, 65, 15–31. <https://doi.org/10.1016/j.geomorph.2004.06.010>
- Berti, M., Corsini, A., & Daehne, A. (2013). Comparative analysis of surface roughness algorithms for the identification of active landslides. *Geomorphology*, 182, 1–18. <https://doi.org/10.1016/j.geomorph.2012.10.022>
- Van Den Eeckhaut, M., Poesen, J., Verstraeten, G., Vanacker, V., Nyssen, J., Moeyersons, J., et al. (2007). Use of LIDAR-derived images for mapping old landslides under forest. *Earth Surface Processes and Landforms*, 32, 754–769. <https://doi.org/10.1002/esp.1417>
- Feizizadeh, B., & Blaschke, T. (2014). An uncertainty and sensitivity analysis approach for GIS-based multicriteria landslide susceptibility mapping. *International Journal of Geographical Information Science*, 28(3), 610–638. <https://doi.org/10.1080/13658816.2013.869821>
- Fiorucci, F., Ardizzone, F., Mondini, A. C., Viero, A., & Guzzetti, F. (2019). Visual interpretation of stereoscopic NDVI satellite images to map rainfall-induced landslides. *Landslides*, 16(1), 165–174. <https://doi.org/10.1007/s10346-018-1069-y>
- Guzzetti, F., Carrara, A., Cardinali, M., & Reichenbach, P. (1999). Landslide hazard evaluation: a review of current techniques and their application in a multi-scale study, Central Italy. *Geomorphology*, 31, 181–216.
- Jones, E. S., Mirus, B. B., Schmitt, R. G., Baum, R. L., Burns, W. J., Crawford, M., et al. (2019). Summary Metadata – Landslide Inventories across the United States. *U.S. Geological Survey Data Release*. <https://doi.org/https://doi.org/10.5066/P9E2A37P>.

- Kritikos, T., Robinson, T. R., & Davie, T. R. H. (2015). Regional coseismic landslide hazard assessment without historical landslide inventories: A new approach. *Journal of Geophysical Research: Earth Surface*, *120*, 711–729. <https://doi.org/10.1002/2014JF003224>
- Lee, S. (2005). Application and cross-validation of spatial logistic multiple regression for landslide susceptibility analysis. *Geosciences Journal*, *9*(1), 63–71. <https://doi.org/10.1007/BF02910555>
- Reichenbach, P., Rossi, M., Malamud, B. D., Mihir, M., & Guzzetti, F. (2018). A review of statistically-based landslide susceptibility models. *Earth-Science Reviews*, *180*(March), 60–91. <https://doi.org/10.1016/j.earscirev.2018.03.001>
- Von Ruetten, J., Papritz, A., Lehmann, P., Rickli, C., & Or, D. (2011). Spatial statistical modeling of shallow landslides-Validating predictions for different landslide inventories and rainfall events. *Geomorphology*, *133*(1–2), 11–22. <https://doi.org/10.1016/j.geomorph.2011.06.010>
- van Westen, C. J., van Asch, T. W. J., & Soeters, R. (2006). Landslide hazard and risk zonation - Why is it still so difficult? *Bulletin of Engineering Geology and the Environment*, *65*, 167–184. <https://doi.org/10.1007/s10064-005-0023-0>

Chapter 2: Development of regional landslide susceptibility models: a first step towards model transferability

Gina Belair^{1,2}, Rebecca Bendick¹

¹ Department of Geosciences, University of Montana, Missoula, Montana, USA

² Current address: U.S. Geological Survey, GHSC, Golden, Colorado, USA

Abstract. Landslides are a globally pervasive problem with the potential to cause significant fatalities and economic losses. Although landslides are widespread, many at-risk regions may not have the high-quality data or resources used in most landslide susceptibility analyses. This study aims to develop regional susceptibility relationships that are versatile and use publicly available data and open-sourced software. Logistic Regression and Frequency Ratio susceptibility relationships were developed in 23 regions in Washington, Utah, North Carolina, and Kentucky, with a region referring to a unique area and data combination. Regions were diverse in their geology, morphology, climate, and nature and quality of their landslide data. The transferability of select models to regions uninvolved in model development was also tested. The transferred models were trained using data from a single region (single-region cross-validation) or a combination of regions (multi-region cross-validation). Potential landslide contributing factors were all derived from a globally available digital surface model while landslide inventories were publicly available from state geological surveys. The contributing factors considered were elevation, slope, aspect, planform curvature, profile curvature, and topographic position index. Models developed using high-quality landslide data delineating scarps, flanks, and individual slope movements performed very well (AUC 0.764 - 0.895; AUC = area under relative operating characteristics curve). Models developed using landslide data dominated by deposits performed less well, but at or near an acceptable level (AUC 0.67 – 0.81). Models developed using older, lower quality landslide data did not perform at an acceptable level (AUC 0.63 – 0.64). The results of testing model transferability had acceptable results for some but not all regions (AUC 0.563 - 0.844). This study is a promising first step in developing generalized landslide susceptibility relationships that can be used in areas that share similar regional scale attributes.

Keywords. landslide susceptibility assessment, logistic regression, frequency ratio, model transferability

1 Introduction

Landslides have the potential to cause a substantial loss of life and damage to infrastructure. The USGS estimates that anywhere between 25-50 annual deaths occur due to landslides in the United States alone, with the death toll in the thousands worldwide (USGS, 2019). Substantial risk still exists due to infrastructure development in landslide-prone areas (Aleotti & Chowdhury, 1999; Schuster & Highland, 2001; and references therein) which enhances demand for effective landslide susceptibility analyses.

This demand has led to a proliferation of methods, both qualitative and quantitative (Aleotti & Chowdhury, 1999; Guzzetti et al., 1999; Reichenbach et al., 2018a; van Westen et al., 2006; and references therein). Qualitative methods may consist of an expert geomorphologist identifying landslide-prone areas in the field (e.g., Carrara & Merenda, 1976; Kienholz, 1978), or by using

index or parameter maps in a geographical information system (e.g., Anbalagan & Singh, 1996; Stevenson, 1977). Qualitative methods can be very useful when past landslide information is not available, but can be too subjective when trying to decide where future slope failures may occur. The majority of new methods being developed and employed are more quantitative. These include geotechnical (e.g., Chowdhury & Zhang, 1993; Wu & Kraft, 1970) and statistical methods (e.g., Budimir et al., 2015; Alberto Carrara, 1983; Neuland, 1976). Geotechnical methods are physics-based slope failure models that are very data intensive and best utilized on single slopes or small areas. Machine learning and statistical methods have increased in use because of their relative objectiveness, but are dependent on the completeness of inventories of past landslide activity in a region (Aleotti & Chowdhury, 1999, and references therein).

Many different contributing factors have been used in statistical landslide susceptibility analyses. In a review of 565 peer-review articles from 1983 to 2016 (Reichenbach et al., 2018), 105 unique variables were found and grouped into 23 unique classes with “slope, geo-lithology, aspect, hydrology, landslide, river/catchment and curvature” accounting for 57% of the all variable occurrences. The number of contributing factors in each assessment is also highly variable, ranging from 2 to 22 variables with an average of 9 variables used. Another review of logistic regression landslide susceptibility analyses found several contributing factors that were common, but did not have a consistent effect, for all landslide types: slope, aspect, elevation, vegetation, lithology, land cover, and distance to drainage (Budimir et al., 2015). These factors are consistent with the current understanding of landslide mechanics (e.g., Hadji et al., 2013; Nilsen et al., 1979; Radbruch-Hall & Varnes, 1976; Soeters & Van Westen, 1996).

Given the importance of gravity in accelerating landslide masses, slope is an important contributing factor both theoretically and empirically (e.g., Baeza & Corominas, 2001; Dehnavi et al., 2015; Kornejady et al., 2017; Kritikos et al., 2015; Pham et al., 2019; Shirzadi et al., 2019; Youssef et al., 2016). Although the significance of other “simple” morphometric variables such as aspect, curvature, relief and elevation have less theoretical and empirical evidence, many studies found these variables to be statistically significant predictors of landslide occurrence (e.g., Conoscenti et al., 2016; Kornejady et al., 2017; Shirzadi et al., 2019).

Data characteristics may confound the use of morphometric factors in susceptibility analysis. For example, digital elevation model (DEM) resolution is one limiting factor in susceptibility analyses, as lower resolution products tend to smooth factor variability. Potential mapping units include pixels, slope units, and unique condition units, with pixels being most commonly used (Reichenbach et al., 2018). Shirzadi et al. (2019) found the best training to testing ratio for a susceptibility analysis is dependent on the resolution of the DEM.

Models highly tuned for a single study area may perform well locally, but poorly outside of the study area. More generalized models may perform less well in a single area, but better in the aggregate. Different approaches applied to a single area may also differ in skill. The majority of susceptibility models are trained in small regions, but some work has been done to develop national and global models (Brabb et al., 1999; Günther et al., 2014; Y. Hong et al., 2007; Kirschbaum et al., 2016; Stanley & Kirschbaum, 2017). The major limitation of these models is their resolution, with the finest resolution being 950 m.

The proliferation of statistical susceptibility analyses necessitates methods for evaluating model quality. Local statistical robustness can be assessed by looking at the effect of different training to testing ratios, persistence of different contributing factors, as well as the effect of variations in input data (Guzzetti, Reichenbach, et al., 2006). Model fit can be assessed using performance criteria such as relative operating characteristic (ROC) curves (Swets, 1988), Peirce skill scores (Peirce, 1884), and Yule's Q scores (Stephenson, 2000; Yule, 1900). These criteria can, with some caveats, be used to compare the skill of different approaches. Most landslide susceptibility analyses do not test the predictive ability of relationships since this can only be done using data that is independent from the training data, either spatially or temporally. In most studies, available data are separated into training and testing regions, but unless these datasets are from a different time or location this only provides information about model fit, not prediction ability. This lack of prediction testing is likely due to the high variability of landslide occurrence between regions, as well as the limitations of landslide inventories that often lack timing information.

Research that does test the predictive ability of susceptibility models is often based on event-triggered landslide inventories. For example, Von Ruetten et al. (2011) found good results when they cross-validated rainfall-induced landslides in the Swiss Alps using three training to testing scenarios: (1) shared geomorphology, (2) shared rainfall event, and (3) different geomorphology and rainfall events. Multiple rainfall-induced susceptibility studies in the Mediterranean found relationships with good predictive ability using multi-temporal landslide inventories (Guzzetti, Galli, et al., 2006; Guzzetti, Reichenbach, et al., 2006) as well as spatially independent landslide inventories (Lombardo et al., 2014). Kritikos et al. (2015) also had positive results when comparing co-seismic landslide occurrence using three separate events and regions. Data from the 1994 Northridge and 2008 Wenchuan earthquakes were combined as a training dataset to test against the landslides induced by the 1999 Chi-Chi earthquake. Cross-validation of relationships for non-event-induced landslides have also been tested. Both Lee (2005) and Domínguez-Cuesta et al. (2007) had good results cross-validating relationships in South Korea and Spain, respectively, while Naranjo et al. (1994) had less favorable results using bivariate statistical methods in Colombia.

This purpose of this study is to progress towards the development of more versatile, generalized regional susceptibility relationships using minimally sufficient and globally available input data. The proposed method was tested in areas diverse in their geology, morphology, climate, and the nature and quality of their landslide data: Washington, Utah, North Carolina and Kentucky. Landslide contributing factors were derived from a 30-m globally available digital surface model and publicly available landslide inventories. We used "simple" morphological variables that were easily calculated and classified in open source software (e.g., R or QGIS). The statistical methods used were also easy to implement and interpret in open source software (e.g., R or Python). The model fit was tested in all regions while statistical robustness was tested in one region. The predictive ability (cross-validation) of select susceptibility relationships in Washington was also tested. This was done using data from single regions, as well as a combination of data from multiple regions. The purpose of this cross-validation is to test whether certain relationships can be used to predict landslide occurrence in regions without inventories. It is unlikely there is a single relationship that can accurately predict landslide occurrence everywhere, but a single relationship could be developed for multiple regions that share large-scale attributes such as climate and

geology. Although this has the potential to oversimplify a very complicated system, it can be used as a first-order approach in regions that lack data and computational resources.

2 Methods

We created empirical models for landslide susceptibility based on readily available global DSMs using logistic regression and frequency ratio methods, following Figure 1. All landslide contributing factors were derived from the *ALOS World 3D – 30 m (AW3D30)* Global Digital Surface Model (Takaku et al., 2014). The derived data layers that represent potential contributing factors for susceptibility are translated into categorical classes for model training and then compared to mapped landslide occurrence to determine weighting coefficients. Model skill was evaluated using four different performance metrics.

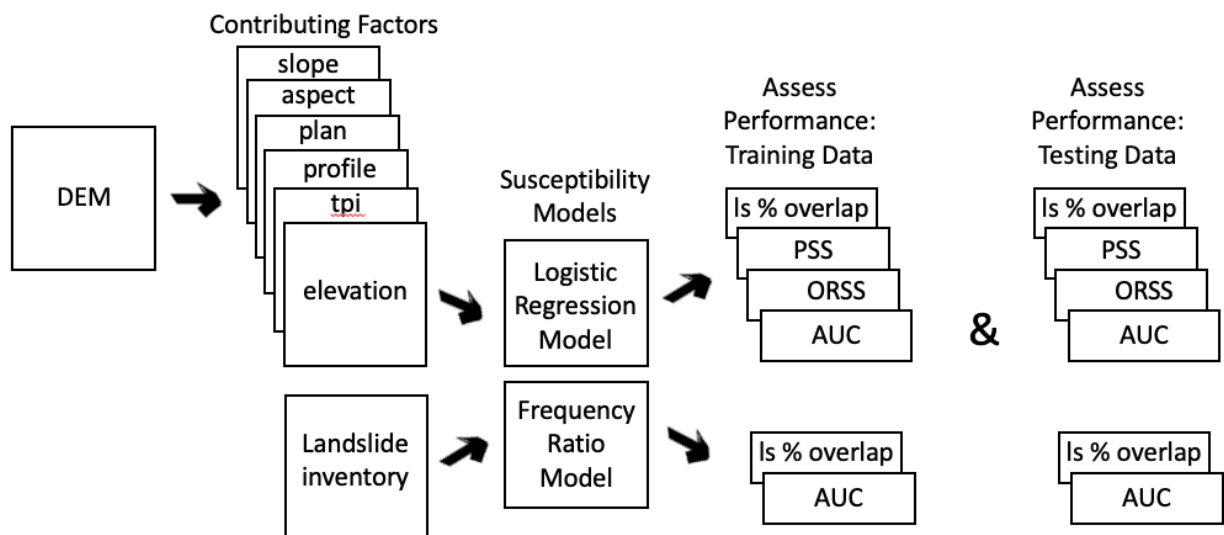


Figure 1. An overview of the methodological approach used in this study. tpi = topographic position index; LS % overlap = percent of landslides in “high”-“very high” susceptibility classes; PSS = Pierce skill score (True skill score); ORSS = Odds ratio skill score (Yule’s Q); AUC = area under relative operating characteristics curve.

2.1 Contributing Factors (independent variables)

We used contributing factors that were derived from a 30 m globally available digital surface model. Other potential factors such as geology, distance to faults, precipitation and soil thickness (Reichenbach et al., 2018) were considered, but were not included since they are not globally available at the desired model resolution. Digital surface models typically capture both natural and built features while digital elevation models represent the bare-Earth. Although a DEM would be more appropriate, the ALOS 30 m DSM was used because it maintains the desired model resolution worldwide (Takaku et al., 2014).

Slope

Many susceptibility studies found slope to be an important landslide contributing factor (e.g., Baeza & Corominas, 2001; Dehnavi et al., 2015; Kornejady et al., 2017; Kritikos et al., 2015; Pham et al., 2019; Shirzadi et al., 2019; Youssef et al., 2016). As slope increases the shear stress

on soil and other unconsolidated materials increases, but the thickness of these unconsolidated materials become negligible at a certain slope angle, so the relationship between landslide hazard and slope is non-linear (Roering et al., 2001). Therefore, the occurrence of shallow slides tends to increase with slope until other mass movements, such as topples and falls, begin to dominate. We derived the slope layer from the DSM using the R 4.0.3 terrain function in the spatialEco package following Horn, 1981 (R Core Team, 2020). Slope was split into 6 classes: 0°-10°, 10°-20°, 20°-30°, 30°-40°, 40°-50°, and >50°.

Elevation

Elevation has also been found to be an important contributing factor in landslide occurrence (e.g., Ayalew et al., 2004; Ayalew & Yamagishi, 2005; Conoscenti et al., 2016; Dehnavi et al., 2015; Hong et al., 2018; Kornejady et al., 2017; Shirzadi et al., 2019). Elevation has potential prognostic utility due to its correlation to more direct causal factors often more difficult to measure. For example, in mountainous terrains elevation is a dominant factor in precipitation patterns (Haiden & Pistotnik, 2009). Elevation is also a factor in the complex feedback of vegetation, soil, and topography (Pelletier et al., 2013). Elevation was split into 7 equal classes ranging from the minimum to maximum elevation.

Aspect

Many studies also found aspect to be an important landslide contributing factor (e.g., Ayalew et al., 2004; Kornejady et al., 2017; Pham et al., 2019; Shirzadi et al., 2019; Youssef et al., 2016). Aspect, like elevation, is a proxy for other landscape characteristics known to influence landslide mechanics such as soil moisture and vegetation, factors that greatly affect soil strength and cohesion (Ray & Jacobs, 2007). These are often climate dependent, so susceptibility as a function of aspect varies from region to region. For example, in three regions in Puerto Rico, cloudiness and wind direction were more important than sun exposure in controlling soil temperature and moisture (Larsen & Torres-Sanchez, 1998). In higher elevation regions, soil moisture and temperature may be more distinct between North and South aspects. We derived the aspect layer from the DSM using the R 4.0.3 terrain function in the spatialEco package following Horn, 1981 (R Core Team, 2020). Aspect was broken up into 4 classes: N (315° - 45°), E (45° - 135°), S (135° - 225°), W (225° - 315°).

Topographic Position Index

Multiple studies found topographic position index (TPI) to be a significant landslide contributing factors (e.g., Conoscenti et al., 2016; Kritikos et al., 2015). TPI is a simple relief measurement that calculates the difference between an elevation value and the mean of the surrounding elevation within a certain radius (Weiss, 2000). The TPI used in this study calculates the difference between a cell and the mean of the surrounding 8 cells using the R 4.0.3 terrain function in the spatialEco package (R Core Team, 2020). The small neighborhood size captures smaller scale features (Jenness et al., 2013). TPI can be used to classify a region into discrete slope position classes, which have been found to be related to various soil properties (e.g., Martz, 1992; Tsui et al., 2004). Positive TPI values indicate the cell is higher than surrounding cells (e.g., ridges) while negative values indicate the cell is lower than in surrounding cells (e.g., valleys) (Weiss, 2000). TPI was broken up into 5 distribution-based classes corresponding to valleys (min to -1sd), lower slopes (-sd to -0.5sd), middle slopes (-0.5sd to 0.5sd), upper slopes (0.5sd to 1sd) and ridges (1sd to max), where sd equals standard deviation.

Plan and Profile Curvature

Plan and profile curvature are used in landslide susceptibility analyses since the curvature of a hillslope affects how water flows above and below the surface. Profile curvature affects flow acceleration, erosion and deposition rates, and soil moisture (Moore et al., 1991; Speight, 1980). Profile or plan curvature were significant predictors in multiple studies (e.g., Ayalew et al., 2004; Chen et al., 2017; Dehnavi et al., 2015; Hong et al., 2018; Kornejady et al., 2017; Shirzadi et al., 2019; Pham et al., 2019). Planform and profile curvature are the second derivatives of elevation in the lateral and vertical direction, respectively. Negative curvature values indicate a concave surface, positive values indicate a convex surface, and zero values indicate a flat slope. Planform and profile curvature were derived from the DSM using the QGIS 3.4.13- SAGA – morphometry package (QGIS Development Team, 2009). Profile and planform curvature variables were each split into three classes: concave (min to -0.001), flat (-0.001 to 0.001), and convex (0.001 to max).

2.2. Landslide Data (dependent variable)

We chose landslide inventories based on their public availability and their variability. The datasets have different quality and resolution. The inventories were also compiled using various methods that include identification from LiDAR-derived DEMs, aerial photographs, stereo-aerial photographs, orthophotos, historical records, and some field verification. Some datasets were also differentiated by landslide type or landslide process domain (e.g., scarps and flanks or deposits).

Kentucky

The Kentucky landslide data were publicly available from the Kentucky Geological Survey (Crawford, 2021). These data include landslides identified from LiDAR-derived DEMs with 1-1.5 m horizontal resolution, but not differentiated by type. Other landslides included in the analysis were earthflows, debris slides and slumps derived from aerial photographs, historical records and field verification between 1977-1981 (Crawford, 2021). Three regions were analyzed in Kentucky with areas ranging from 490 to 10970 km². Study areas 1 and 2 were processed using landslides derived from both LiDAR and aerial methods (ky1 and ky2), while area 1 was also processed using landslides from aerial methods alone (ky1a). Study areas 2 and 3 were also analyzed using only LiDAR-derived landslide data (ky21 and ky31).

North Carolina

The North Carolina landslide data were publicly available from the North Carolina Geological Survey (North Carolina Geological Survey, 2021). These data include individual slope movements identified from aerial photography, orthophotography, and field verification. Landslide deposits that consist of earth, debris, and rock fragments were also included in the analysis. The North Carolina study area spanned roughly 6016 km². This area was processed using just individual slope movements (nc1sm), deposits (nc1d), and the combination of individual slope movements and deposits (nc1).

Utah

The landslide data for Utah were publicly available from the Utah Geological Survey (Utah Geological Survey, 2016). These landslides were identified using LiDAR and stereo-aerial photography with some field verification. These data include rotational slides, translational slides,

and flows at a scale of 1:24,000 or better, with some slide types unidentified. The Utah study area spanned roughly 1082 km². This area was processed using landslides scarps (ut1s), deposits (ut1d), and a combination of both (ut1).

Washington

The landslide data for Washington were publicly available from Washington Geological Survey (Washington Geological Survey, 2020). The landslides used were all detected using LiDAR derived DEMs. One subset of data delineates the scarps and flanks, another delineates landslide deposits, and another delineates an entire landslide area that includes scarps, flanks, and deposits (Washington Geological Survey, 2020). Four areas were analyzed in Washington ranging from 233 km² to 2149 km². We analyzed regions 1-4 using all three datasets together (wa1-4), just the scarps and flanks (wa1-4sf), and just the deposits (wa1-4d).

2.3 Statistical Relationships

2.3.1 Logistic Regression

Logistic regression is a common method used in landslide susceptibility analyses (e.g., Budimir et al., 2015; Hong et al., 2016; Shahabi et al., 2014; Yalcin et al., 2011). In binary logistic regression, the parameters of the logistic model are estimated using the maximum likelihood method which maximizes the ratio of the probability an event occurred to the probability the event did not occur. The dependent variable is binary; in landslide susceptibility analyses this is whether a landslide occurred or not. The independent variables (i.e., landslide contributing factors) can be discrete, continuous, or a combination of both and do not need to be normally distributed. The predicted value is the probability of landslide occurrence ranging from 0 to 1. The logistic function shown below represents the probability of the event occurring.

$$P(\text{landslide}) = \frac{1}{1 + e^{-z}}$$

$$z = \beta_0 + \beta_1 x_1 + \beta_2 x_2 + \dots + \beta_n x_n$$

$P(\text{landslide})$: probability of the event (landslide) occurring

β_i ($i = 0, 1, 2, \dots, n$): parameters of the i_{th} variable

x_i ($i = 0, 1, 2, \dots, n$): values of the i_{th} independent variable

2.3.2 Frequency Ratio

Frequency Ratio is another common statistical method used in landslide susceptibility analyses (e.g., Aditian et al., 2018; Hong et al., 2016; Shahabi et al., 2014; Yalcin et al., 2011). This method uses the ratio of landslide density of the contributing factors to the landslide density of the total region. Each explanatory variable is broken up into representative classes. The landslide density of each variable class is the landslide area in that class as a fraction of the total class area. The landslide density of the region is the total landslide area as a fraction of the total study area. Frequency ratio values above 1 contribute positively to landslide occurrence while frequency ratio values below 1 are the opposite. Landslide Susceptibility Index (LSI) values are calculated by summing the frequency ratios that correspond to the appropriate explanatory variable class. Relative probability of landslide occurrence is then found by normalizing the LSI values.

$$FR_{ij} = \left(\frac{N_{ij}}{A_{ij}} / \frac{N_r}{A_r} \right)$$

$$LSI = FR_1 + FR_2 + \dots + FR_n$$

$$P(true) = \frac{LSI - \min(LSI)}{\max(LSI) - \min(LSI)}$$

FR_{ij} : frequency ratio of j_{th} class of i_{th} response variable

N_{ij} : area of landslides in j_{th} class of i_{th} response variable

A_{ij} : area of j_{th} class of i_{th} response variable

N_r : total area of landslides

A_r : total study region area

LSI : Landslide Susceptibility Index of each pixel

2.4 Model Building and Validation

Empirical susceptibility relationships were determined for all regions, shown in Figure 2 and Table 1, using both logistic regression and frequency ratio methods. In this paper, a region refers to a unique area and landslide data combination (e.g., region wa1sf refers to Washington area 1 using only scarps and flanks landslide data). We cross-validated select logistic regression models on regions independent from training; this will be referred to as single-region cross-validation (SRCV). This was done in Washington areas 1 – 4 using the scarps and flanks landslide data (e.g., model LR-wa1sf was used to predict susceptibility in regions wa2sf, wa3sf, and wa4sf). We also developed logistic regression models using data from a combination of regions and cross-validated them on independent regions, this will be referred to as multi-region cross-validation (MRCV). This analysis was performed in Washington areas 1 – 3 using the scarps and flanks landslide data (e.g., a LR model developed from data in wa1sf and wa2sf was used to predict susceptibility in region wa3sf). We used two different methods of data classification, contributing factors from each region were either classified before they were combined (separate) or after they were combined (together). All relationships were determined using a training dataset that consisted of 70 percent of landslides pixels with an equal number of randomly selected non-landslide pixels. A simplified workflow of each of these analyses is shown in Figure 3. We classified the final susceptibility predictions into five classes using three techniques: Jenks natural breaks, equal intervals ranging from minimum to maximum susceptibility, and equal intervals ranging from 0 to 1. The five susceptibility classes correspond to “low”, “low-moderate”, “moderate”, “high”, and “very-high” susceptibility.

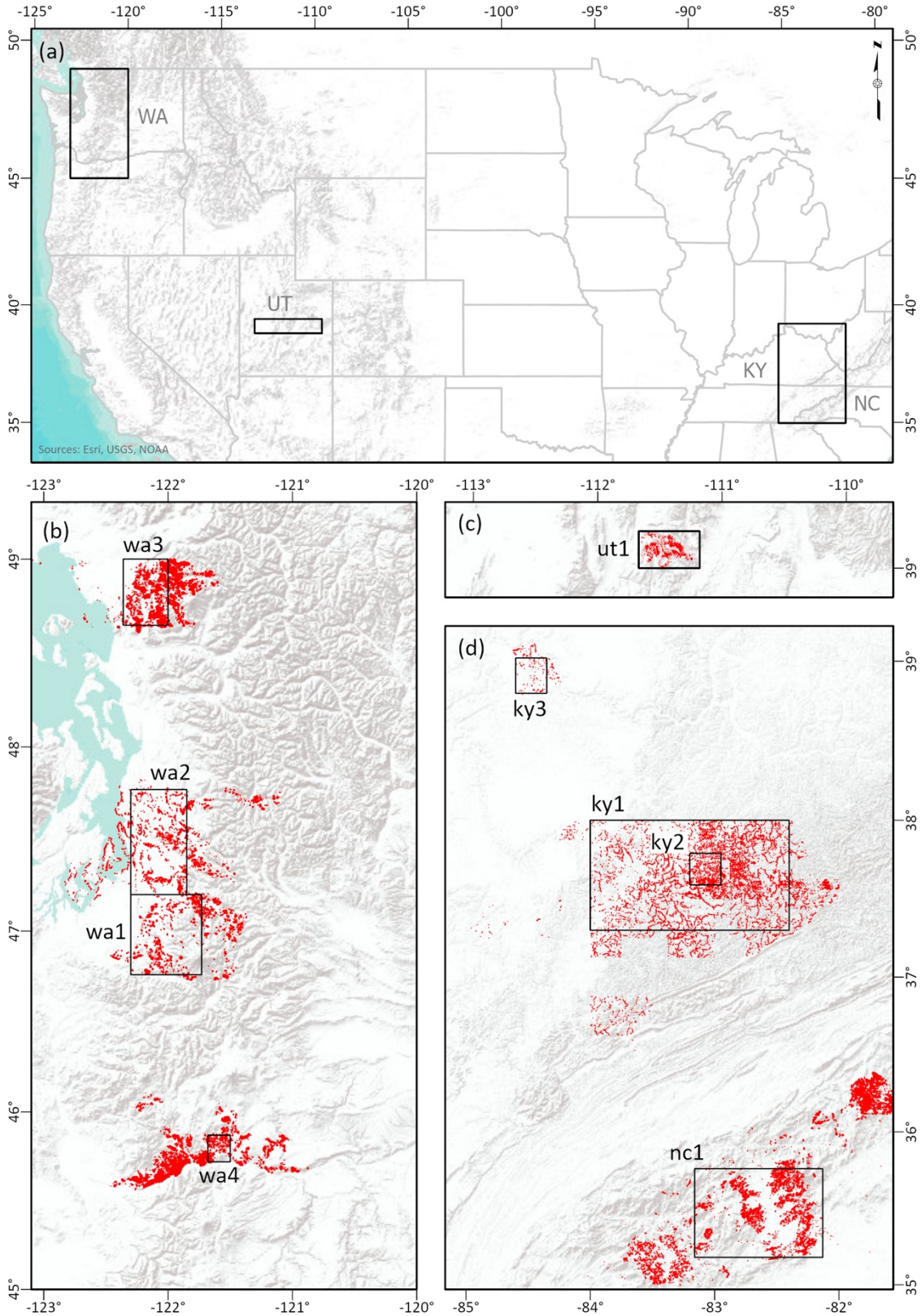


Figure 2. Study regions. Landslides shown in red. (a) Overview showing location of larger study areas; (b) Washington areas; (c) Utah area; (d) Kentucky and North Carolina areas. Note that (b) – (d) share the same scale. (Coordinate System: WGS 1984 Web Mercator Auxiliary Sphere)

Region	Extent (WGS 1984)	Study Area (km ²)	Landslide Area (km ²)	Landslide Data Description
wa1sf	(-122.3, -121.73, 4.7, 47.2)	2121	7	Scarps & Flanks
wa2sf	(-122.3, -121.85, 47.2, 47.77)	2149	12	Scarps & Flanks
wa3sf	(-122.36, -122, 48.65, 49)	1029	14	Scarps & Flanks
wa4sf	(-121.68, -121.5, 45.72, 45.8)	233	4	Scarps & Flanks
wa1d	(-122.3, -121.73, 4.7, 47.2)	2121	47	Deposits
wa2d	(-122.3, -121.85, 47.2, 47.77)	2149	63	Deposits
wa3d	(-122.36, -122, 48.65, 49)	1029	151	Deposits
wa4d	(-121.68, -121.5, 45.72, 45.8)	233	22	Deposits
wa1	(-122.3, -121.73, 4.7, 47.2)	2121	83	Scarps & Flanks & Deposits
wa2	(-122.3, -121.85, 47.2, 47.77)	2149	76	Scarps & Flanks & Deposits
wa3	(-122.36, -122, 48.65, 49)	1029	165	Scarps & Flanks & Deposits
wa4	(-121.68, -121.5, 45.72, 45.8)	233	26	Scarps & Flanks & Deposits
ut1s	(-111.67, -111.18, 39, 39.23)	1082	8	Scarps
ut1d	(-111.67, -111.18, 39, 39.23)	1082	243	Deposits
ut1	(-111.67, -111.18, 39, 39.23)	1082	252	Scarps & Deposits
ky1	(-84, -82.4, 37.3, 38)	10970	60	LiDAR & Aerial
ky1a	(-84, -82.4, 37.3, 38)	10970	53	Aerial
ky2	(-83.2, -82.95, 37.59, 37.79)	489	10	LiDAR & Aerial
ky2l	(-83.2, -82.95, 37.59, 37.79)	489	5	LiDAR
ky3l	(-84.6, -84.35, 38.8, 39.02)	530	2	LiDAR
nc1sm	(-83.16, -82.13, 35.18, 35.76)	6016	4	Slope movements
nc1d	(-83.16, -82.13, 35.18, 35.76)	6016	146	Deposits
nc1	(-83.16, -82.13, 35.18, 35.76)	6016	149	Slope Movements & Deposits

Table 1. Summary of the study regions, the locations of which are shown in Figure 1. A region refers to a unique area and landslide data combination.

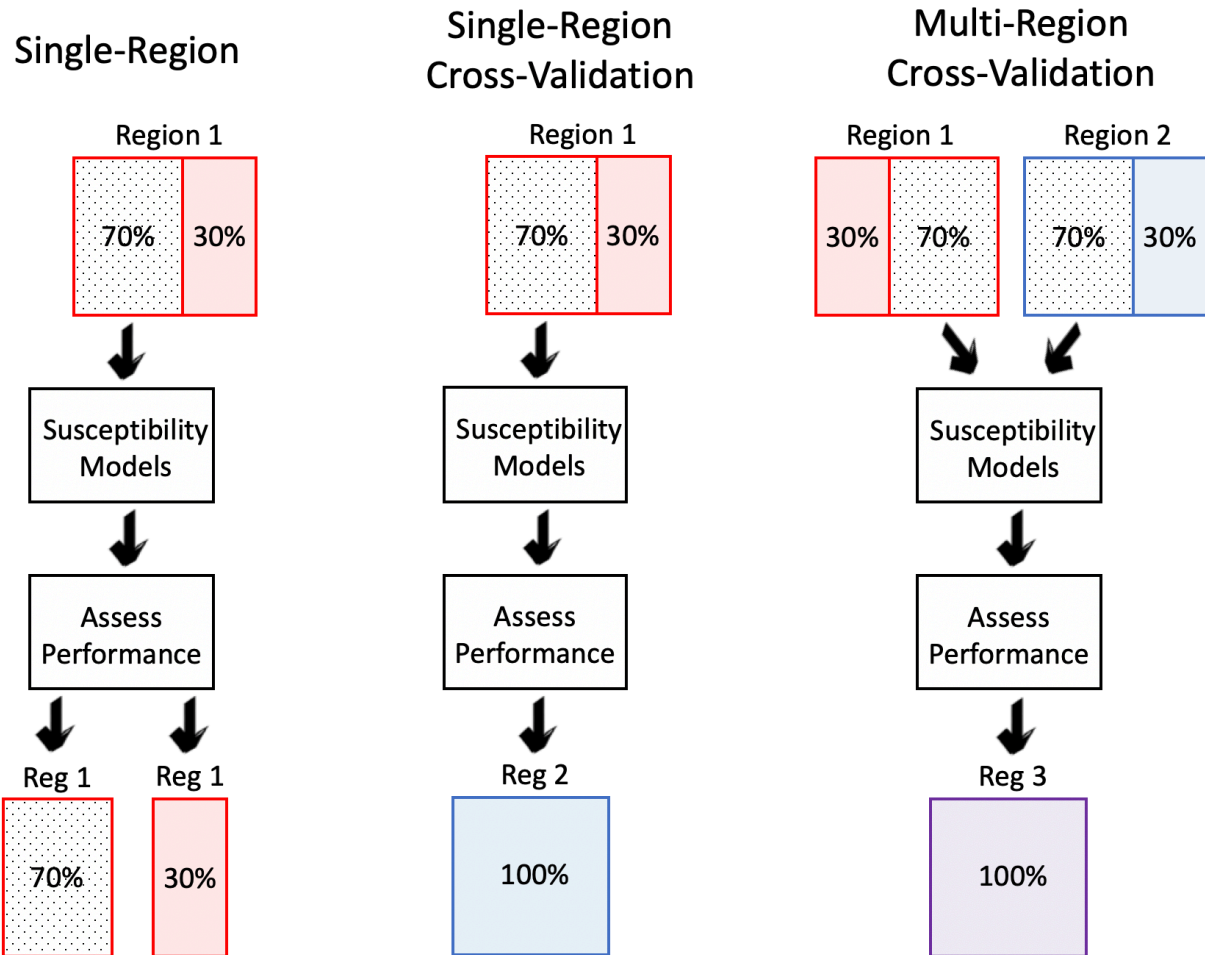


Figure 3. Overview of workflows used for developing and assessing susceptibility relationships. Single-region analysis was conducted in all 23 regions, single-region cross-validation was conducted in four regions (wa1-4sf), multi-region cross-validation was conducted in three regions (wa1-3sf).

To test whether landslide occurrence is dependent on the contributing factors, we extracted the statistical significance of each factor from the logistic regression model equation. Statistical significance is determined from a p-value, the probability that the result, in this case the effect the contributing factor has on landslide occurrence, is just due to chance (R Core Team, 2020). A p-value below 0.05 is often accepted as very strong evidence that the effect is not due to chance. It should be noted that this significance shows whether a factor provides systematic information about landslide occurrence, not necessarily whether the factor positively or negatively affects the occurrence. Multicollinearity, the interdependency between explanatory variables, can be a problem in regression analyses since explanatory variables are expected to be independent (Farrar & Glauber, 1967). We tested the degree of multicollinearity between factors by calculating the variance inflation factor (VIF), which measures whether a predictor can be linearly estimated by the others (R Core Team, 2020). A strict cutoff for the VIF value is not recommended, but it is often suggested that VIF values above 5 or 10 suggest a problematic level of multicollinearity (Craney & Surlles, 2002).

We used multiple methods to evaluate the performance of the models. Relative operating characteristic (ROC) curves, the true-positive rate versus the false-positive rate, were used to assess the accuracy of the assessments (Swets, 1988). ROC curves are useful when the cutoff probability that determines a true or a false is unclear. The area under the ROC curve (AUC) is a common metric used to assess the accuracy of binary systems. An AUC of 0.5 shows no signs of predictive ability while AUC values closer to 1 signify higher performance. Model performance is classified as acceptable, excellent, and outstanding for AUC thresholds of 0.7, 0.8, and 0.9, respectively (Conoscenti et al., 2016; Hosmer & Lemeshow, 2000). The susceptibility relationships were also assessed using the cutoff-dependent criteria shown in Table 2, which include the Pierce skill score (PSS; Peirce, 1884) and Yule's Q score (ORSS; Stephenson, 2000; Yule, 1900). These metrics range from -1 to 1 and take all values of a contingency table into account (i.e., true positives, true negatives, false positives, and false negatives). Zero scores correspond to random no-skill prediction ability, while values closer to 1 indicate higher prediction ability. We chose a cutoff value of 0.5 to differentiate between stable and unstable slopes, due to its statistical meaning. The percentage of landslides correctly classified in high or very-high susceptibility classes (LS % overlap) was also used to assess the methods.

Pierce skill score (True skill score)	$\frac{tp}{tp + fn} - \frac{fp}{fp + tn}$
Odds ratio skill score (Yule's Q)	$\frac{tp \cdot tn - fp \cdot fn}{tp \cdot tn + fp \cdot fn}$

Table 2. Cutoff dependent accuracy statistics. tp = true positive, tn = true negative, fp = false positive, fn = false negative

We performed a sensitivity analysis to determine the effect of using random training data. The analysis was performed in the same region (wa2sf) using 50 randomly selected training datasets (see Figure S2 in supplement). The importance of the percent of landslides in the training dataset was also considered using different training to testing ratios of 60%:40% and 80%:20% (see Figure S1 in supplement).

3. Results

We extracted the statistical significance of each contributing factor from the logistic regression models. This statistical significance is a measure of whether the effect the contributing factor has on landslide occurrence is real or due to random chance. 21 of the 23 regions found west-facing aspect to be a significant predictor of landslide occurrence ($p < 0.05$). 21 of the 23 regions found elevations in the second class to be a significant predictor of landslide occurrence ($p < 0.05$). 16 of the 23 regions found convex planform and convex profile curvatures to be a significant predictors of landslide occurrence ($p < 0.05$). 14 of the 23 regions found slopes from 0-10° and 10-20° to be significant predictors of landslide occurrence ($p < 0.05$). All 23 regions found the TPI values in the fourth class to be significant predictors of landslide occurrence ($p < 0.05$). These results are summarized in Table 3. No multicollinearity was found for any of the landslide contributing factors in any region. The variance inflation factors of all the variables were below 1.445 (see Table S2 in supplement), which is well under the problematic VIF of 5 or larger.

Landslide Contributing Factor	Number of regions factor was significant
aspect	21
elevation	21
planform curvature	16
profile curvature	16
slope	14
tpi	23

Table 3. Number of regions (out of 23) that found each contributing factor to be a significant predictor of landslide occurrence using a cutoff p-value of 0.05.

The area under the relative operating characteristic curves (AUC) for the logistic regression and frequency ratio relationships for both the training and testing datasets are shown in Table 4 and select ROC curves are shown in Figure 4. According to the AUC performance criteria (0.7 – 0.8 acceptable, 0.8 – 0.9 excellent, > 0.9 outstanding), the majority of models performed at or above an acceptable level. Models with high quality data differentiated by landslide process domain or by individual slope movements performed best. These include Washington models that used only scarps and flanks data, Utah scarps data, or North Carolina individual slope movements (wa1-4sf, ut1s, nc1sm). AUC values for the logistic regression training data ranged from 0.764 - 0.895 with an average of 0.83. All models that used just deposits data, or a combination of scarps, flanks and deposits data (i.e., wa1-4d, wa1-4, ut1d, ut1, nc1d, and nc1) performed less well but still mostly met the acceptable level. AUC values for the logistic regression training data ranged from 0.67 – 0.81 with an average of 0.717. In Kentucky, the models that used a substantial portion of LiDAR-derived landslides (i.e., ky2, ky2l, and ky3l) performed at an acceptable or excellent level with AUC values from 0.750 - 0.847 for LR training data. In Kentucky, the models dominated by aerial derived landslides (i.e., ky1 and ky1a, mapped and verified between 1977-1981) did not perform well with AUC values from 0.63 - 0.64 for LR training data. In all regions, logistic regression and frequency ratio models had similar AUC values. Logistic regression always had slightly higher AUC values than frequency ratio, but FR AUC values were all within 0.033 of their respective LR AUC values. For all regions, the difference between AUC values of the training and testing datasets were all within 0.017.

The Pierce skill score (PSS) and the Yule’s Q score (ORSS) for the logistic regression models are shown in Table 4. These values were not calculated for the frequency ratio relationships since there is no statistically significant cut-off value that differentiates between a success or failure (i.e., landslide presence or absence) for this type of relationship. For logistic regression this cut-off is 0.5. For all relationships these values behaved similarly to the AUC values; this behavior can be seen in Figure 5. The PSS values range from 0.189 – 0.624, while the ORSS values range from 0.369 – 0.898.

Region	Logistic Regression				Frequency Ratio	
	Train AUC	Test AUC	PSS	ORSS	Train AUC	Test AUC
wa1sf	0.836	0.823	0.528	0.856	0.807	0.790
wa2sf	0.864	0.860	0.569	0.860	0.849	0.842
wa3sf	0.808	0.806	0.476	0.790	0.805	0.801
wa4sf	0.764	0.753	0.366	0.657	0.759	0.746
ut1s	0.895	0.896	0.624	0.898	0.881	0.884
nc1sm	0.811	0.806	0.469	0.769	0.797	0.792
wa1d	0.730	0.721	0.326	0.603	0.720	0.711
wa2d	0.803	0.802	0.489	0.790	0.795	0.794
wa3d	0.716	0.712	0.311	0.576	0.709	0.705
wa4d	0.682	0.677	0.268	0.517	0.677	0.672
ut1d	0.698	0.698	0.296	0.548	0.695	0.694
nc1d	0.703	0.703	0.297	0.548	0.694	0.695
wa1	0.692	0.692	0.296	0.555	0.688	0.688
wa2	0.810	0.811	0.497	0.798	0.801	0.802
wa3	0.722	0.721	0.332	0.611	0.715	0.714
wa4	0.670	0.672	0.251	0.478	0.664	0.664
ut1	0.685	0.685	0.275	0.514	0.683	0.683
nc1	0.698	0.698	0.289	0.536	0.689	0.689
ky1	0.630	0.629	0.189	0.369	0.624	0.622
ky1a	0.640	0.636	0.209	0.401	0.637	0.633
ky2	0.750	0.751	0.389	0.685	0.740	0.743
ky2l	0.765	0.758	0.394	0.683	0.756	0.749
ky3l	0.847	0.830	0.558	0.851	0.837	0.832

Table 4. Diagnostic statistics with no qualitative user input. Cutoff-independent AUC values. Cutoff-dependent (0.5 indicates cutoff between stable and unstable slopes) criteria PSS and ORSS.

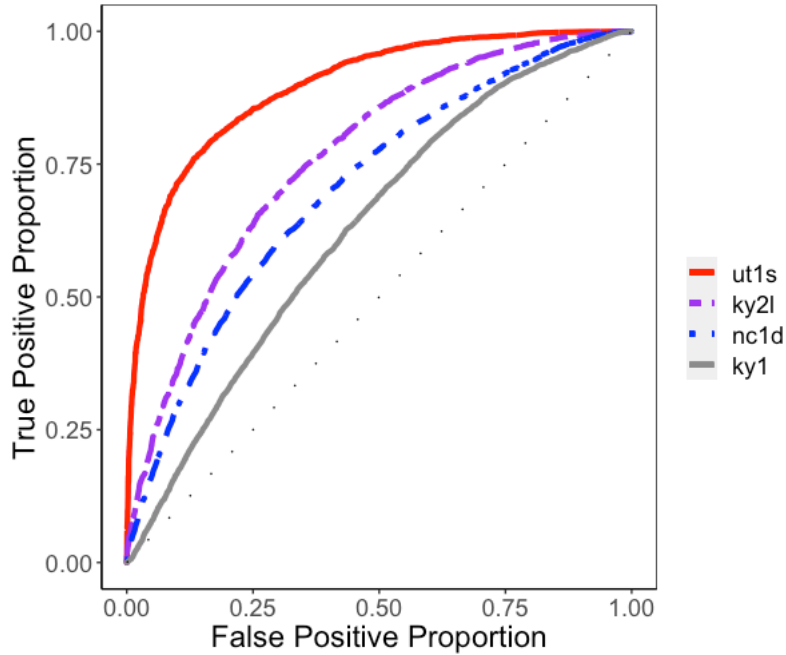


Figure 4. Select ROC curves of different types of regions. The diagonal line represents random, no information results. ut1s shows the best performance of the ensemble, while ky1 shows the worst. ut1s is “scarps, flanks, individual slope movements”; nc1s is “dominated by deposits data”; ky1 is “dominated by aerial-derived landslides”; ky2l is “dominated by lidar-derived landslides.”

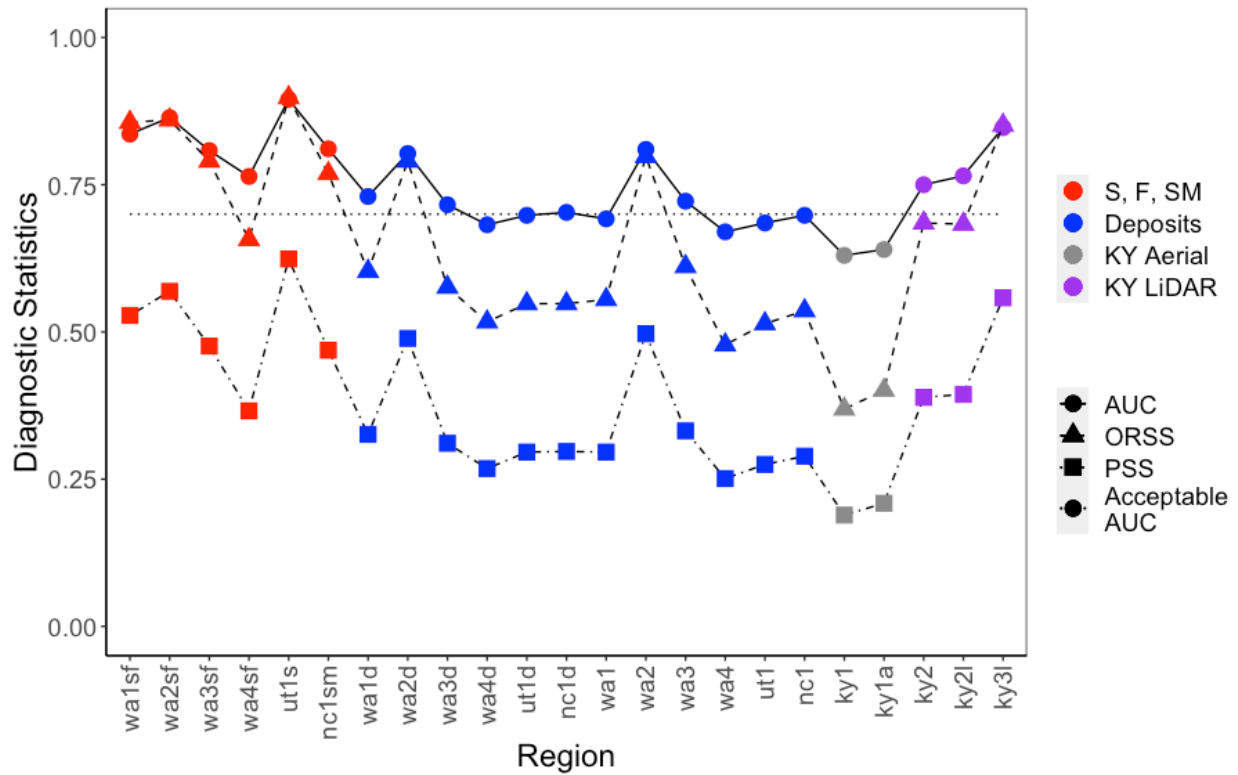


Figure 5. Plot of logistic regression diagnostic statistics. “KY LiDAR” and “S, F, SM” regions consistently outperform “KY Aerial” and “deposits” regions for all diagnostic statistics shown.

AUC = area under relative operating characteristics curve; PSS = Pierce skill score (True skill score); ORSS = Odds ratio skill score (Yule's Q); Acceptable AUC = "acceptable" performance with AUC values above 0.7. "S, F, SM" = scarps, flanks, individual slope movements; "deposits" = dominated by deposits data; "KY Aerial" = dominated by aerial-derived landslides; "KY LiDAR" = dominated by lidar-derived landslides.

The overlap between landslide susceptibility classes and landslide occurrence for all regions is shown in Table S1 (see supplement). An example susceptibility map for region wa2sf is shown in Figure 6. This is a logistic regression model using an equal (0 - 1) classification method for susceptibility. The classification method that provides the best results is dependent on region, but should capture a large number of landslides in the "high" – "very high" susceptibility classes without making those areas too large. For logistic regression the percentage of landslides in the "high" – "very high" susceptibility classes ranged from 49.7% - 84.6%, 57.5% – 84.6%, and 20.2% - 77.8% for Jenks, equal (min – max), and equal (0 – 1) classification methods respectively. For frequency ratio the percentage of landslides in the "high" – "very high" susceptibility classes ranged from 51.6% - 95.7%, 59.9% – 91.7%, and 96.6% - 100% for Jenks, equal (min – max), and equal (0 – 1) classification methods respectively. The frequency ratio results for the equal (0 - 1) classification method are misleading, although a large portion of the landslides are captured, anywhere from 58.9% - 100% of the study area falls within the "high" – "very high" susceptibility classes.

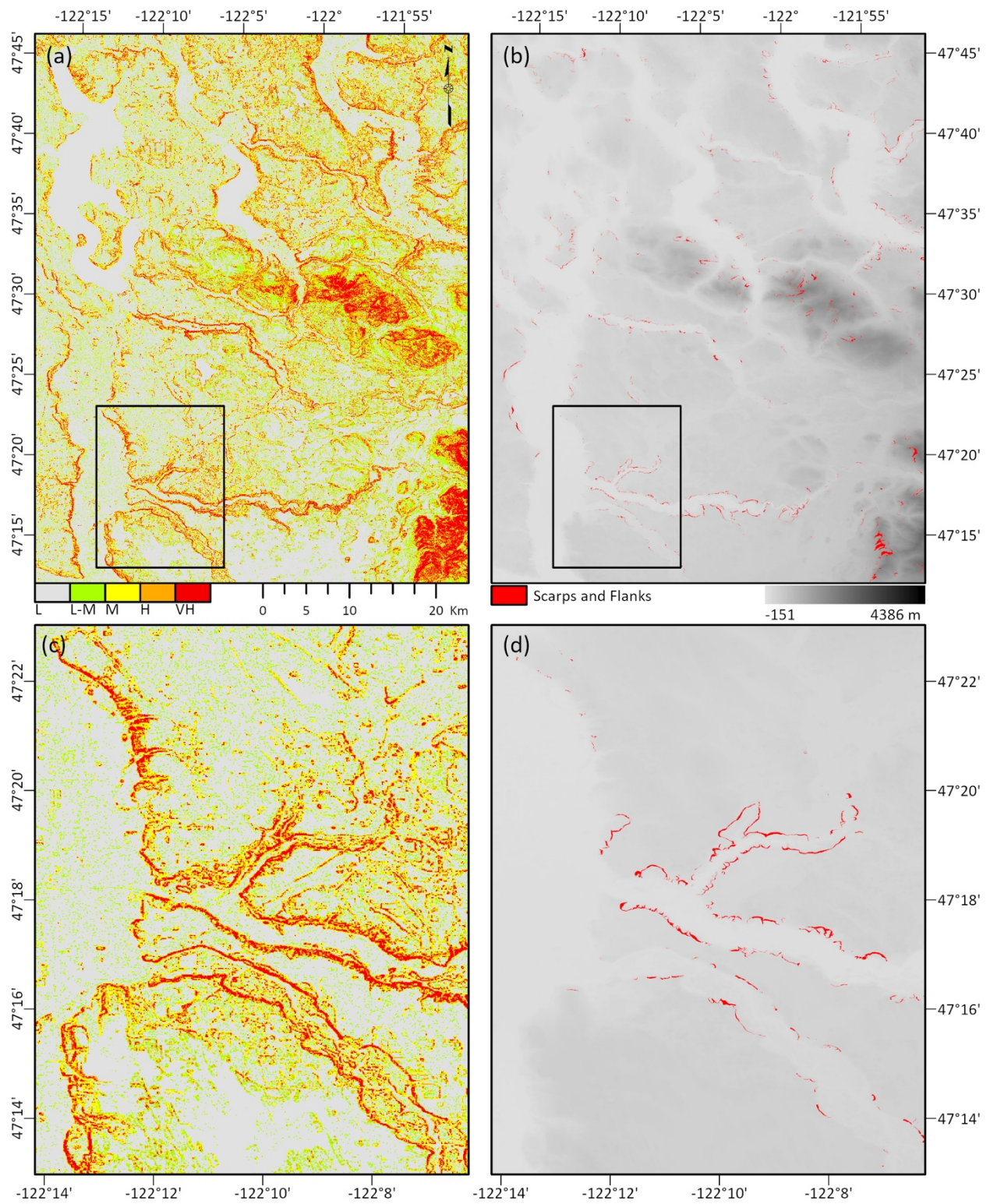


Figure 6. (a) Susceptibility map of wa2sf region using logistic regression model. L = Low, L-M = Low – Moderate, M = Moderate, H = High, VH = Very High. Susceptibility was classified using the equal (0 – 1) classification method. (b) Landslide occurrence map overlapping elevation. (c) Susceptibility map of sub-region. (d) Landslide occurrence map of sub-region.

The cross-validation results are more variable. The PSS, ORSS, and AUC values for single-region-cross-validation (SRCV) and multi-region-cross-validation (MRCV) are shown in Table 5 and Table 6, respectively. The SRCV results using data trained and tested between regions wa2sf, wa3sf, and wa4sf had acceptable prediction success (AUC: 0.714 – 0.785, PSS: 0.187 – 0.383, ORSS: 0.613 – 0.787). The SRCV results that were trained or tested on region wa1sf had poor results with the exception of the model trained in wa2sf (AUC: 0.563 – 0.741, PSS: {-0.068} - 0.366, ORSS: {-0.484} - 0.708). The MRCV results using data classified separately performed better than when data was classified together (Separately: AUC: 0.678 – 0.844, Together: AUC 0.574 – 0.676).

Logistic Regression				
Train	Test	AUC	PSS	ORSS
wasf1	wasf2	0.636	0.358	0.680
	wasf3	0.579	0.028	0.067
	wasf4	0.600	-0.062	-0.457
wasf2	wasf1	0.741	0.366	0.708
	wasf3	0.750	0.383	0.742
	wasf4	0.721	0.305	0.717
wasf3	wasf1	0.607	0.033	0.074
	wasf2	0.777	0.282	0.707
	wasf4	0.714	0.334	0.658
wasf4	wasf1	0.563	-0.068	-0.484
	wasf2	0.725	0.187	0.787
	wasf3	0.785	0.279	0.613

Table 5. Diagnostic statistics from single-region-cross-validation (SRCV): testing logistic regression models on regions not included in training. The values are found using 100% of data in testing regions.

Data	Train	Test	AUC	PSS	ORSS
Classified Separately	wasf1, wasf2	wasf3	0.678	0.226	0.431
	wasf1, wasf3	wasf2	0.844	0.471	0.817
	wasf2, wasf3	wasf1	0.691	0.333	0.622
Classified Together	wasf1, wasf2	wasf3	0.574	0.325	0.726
	wasf1, wasf3	wasf2	0.660	0.040	0.095
	wasf2, wasf3	wasf1	0.676	0.321	0.605

Table 6. Diagnostic statistics from multi-region-cross-validation (MRCV): testing logistic regression models on regions not included in training. Training data were either classified before (separately) or after (together) combination. The values are found using 100% of data in testing regions.

4. Discussion

In landslide susceptibility analyses, there are subjective decisions to make that often depend on the amount and quality of available data and level of expertise of the practitioner. These decisions include the type of relationship determined, the nature and number of contributing factors, the type of mapping unit used, the ratio of training to testing data, and how to classify susceptibility. Compiling accurate landslide inventories is often time-consuming and resource-heavy. Most newly developed techniques are computationally expensive, specific to limited study areas, and use data that can be hard to obtain. At the same time, places with substantial landslide hazard may not have the resources to obtain high-quality, high-resolution data or perform complex statistical analyses. Overfitting is a pervasive problem in landslide susceptibility analyses.

We aim to develop a method that is easy to implement and reduces the number of decisions and technical investments the practitioner needs to make. We use a 30-m globally available DSM, publicly available landslide inventories, and open-source software packages R and QGIS. Contributing factors were all derived from a DSM and were automatically broken into their respective classes. We tested the method using landslide data of various quality in diverse regions. The more general a method is, the more likely the relationships can be used to determine susceptibility in other regions; this study is a first step in this pursuit. If general relationships can be used to predict susceptibility in other regions, this would allow susceptibility to be determined in places without landslide inventories. The models performed well in most regions diverse in their climate, geology, quality of data, extent of study area, and the area of landslides. We also found that some relationships developed in one region, or a combination of regions, had good predictive performance in other regions. This result indicates the potential transferability of relationships under certain circumstances.

Although the Frequency Ratio (FR) relationships have good predictive performance based on AUC values, Logistic Regression (LR) is the preferred method. Logistic regression is more statistically rigorous. The output of LR is already a percentage likelihood while normalized FR values are relative and can only be interpreted in relation to the region used to determine them. The statistical significance of factors can be easily extracted from the LR equation and other cut-off-based criteria are applicable to LR relationships, which is not true for FR relationships. After normalization, the FR relative susceptibility values in this study are very high, with the first quantile values of the relationships ranging from 0.564 to 0.867. It is still possible to determine susceptibility from FR relationships, but the user should be careful interpreting these values and assigning susceptibility classes. It is only slightly more difficult to interpret the results of LR compared to FR, but the benefits outweigh this increased difficulty.

It is important to carefully consider what factors should be included in a model since factors may be found to be statistically significant predictors of landslide occurrence, but might not be of practical importance. We considered factors with strong theoretical or empirical evidence that directly connects them to landslide occurrence, or as proxies to factors more directly linked to landslide occurrence such as erosion and deposition rates, and soil moisture. VIF values for all variables in all regions were 1.445 or less, which shows there is no multicollinearity between predictors. A majority of regions (14 of 23) found at least one class of each contributing factor to be statistically significant ($p < 0.05$). If even one class of a contributing factor is found to have

predictive power, all classes should be included in order to calculate susceptibility in every range of factor values. Although not every region found all contributing factors to be important, all factors should be included in a preliminary model. Further analysis could be conducted by gradually removing predictors not found to be significant, a method known as backward stepwise regression. Backward stepwise regression was not done in this study; even without the removal of irrelevant factors the models still perform at an acceptable level.

In this study, there was not one best way to break up susceptibility into classes. Three methods were used: Jenks natural breaks, equal breaks (min – max), and equal breaks (0 – 1). Jenks and equal breaks (min – max) are dependent on the distribution of susceptibility and since this distribution is relative, the classified susceptibility should not be used to compare to other regions. Equal breaks (0 – 1) are not dependent on the distribution of susceptibility, so the classified susceptibility can be compared to other regions. Careful consideration is needed when breaking up susceptibility into classes. It is important to capture as many landslides as possible in high susceptibility classes, without increasing the area of these classes too much. Even if you capture most of the landslides, this will not provide useful information if the majority of a region is considered high susceptibility. Since Frequency Ratio values were normalized they provide relative susceptibility and should not be compared to other regions. For the majority of regions, the median FR value is very high, so the results should be carefully considered.

We expect that regions with high quality landslide data distinguished by landslide process domain will perform well. The locations of scarps and flanks provide information on where landslides are likely to originate, while the location of deposits provides information on where landslides have traveled as well as where possible reactivation of landslides may occur. Scarps and flanks data and deposits data both contain important, but unique information about landslide susceptibility. When possible, to increase the usefulness of each dataset, they should be considered separately. This can be evidenced by the predictive performance of relationships determined from different datasets in Washington, Utah, and North Carolina. The data that describes the scarps, flanks and individual slope movements performed the best (LR AUC 0.764 - 0.895). Data that describes landslide deposits or a combination of scarps, flanks and deposits performed well, but had less predictive ability (LR AUC 0.67 – 0.81). The difference in performance between landslide source data and deposits data is likely due to the large difference in landslide area and the more variable nature of deposits. In Washington, Utah, and North Carolina the area of deposits was anywhere between 5-33 times larger than the area of landslide sources (5-11, 29, and 33 respectively). This larger area, as well as the nature of deposits leads to more variability in the distribution of deposits within each variable class.

The quality of landslide inventories was found to be an important control on model performance. The majority of inventories used in this analysis are identified from LiDAR derived DEMS, while a smaller portion of landslides were identified using aerial photographs, stereo-aerial photographs, orthophotos, historical records, and field verification. Although accuracy of each identification method depends on factors such as landslide age, landslide size and vegetation cover, we consider high quality inventories to be compiled using more accurate methods such as identification from LiDAR-derived DEMs and stereo-aerial photographs. In Kentucky, regions dominated by LiDAR-derived landslide data performs well (ky2, ky2l, ky3l: LR AUC 0.75 – 0.847). Relationships that were dominated by aerial-derived landslide data did not perform well (ky1, ky1a: LR AUC 0.629

– 0.64). The reduced performance of regions dominated by aerial-derived landslides is likely due to the quality of this specific dataset. This dataset is based on aerial photographs, historical records, and field verification between 1977-1981 with a confidence in nature and extent of only 3 out of 8 (Crawford, 2021). This is not to say non-LiDAR identified landslides cannot be used since the North Carolina inventory includes aerial derived landslides, but still performs well. This difference is likely due to the age and nature of the KY data that may not be accurate to the current landscape. Although this method works well in a variety of situations, care should be taken when using this method on landslide inventories of questionable quality.

The method may not perform consistently at all scales. It performed the best at regional scales, multi-county in size, which is an appropriate scale for disaster planning purposes. This can be seen in the slightly reduced predictive performance for all datasets in Washington region 4, a region spanning only $\sim 230 \text{ km}^2$. This method should also not be used at a national scale since there would be too much variation in topography, climate, and the nature of the landslides.

There were promising results when relationships trained in one region were used to predict susceptibility in other regions. This was tested using single-region and multi-region cross-validation using the Washington scarps and flanks data. SRCV logistic regression models trained and tested in regions 2, 3, or 4 had good predictive performance, while results using testing or training data in region 1 did not have acceptable performance, as seen in Table 5. MRCV logistic regression models in wa1-3sf had acceptable performance when data was classified separately, as seen in Table 6. This could be due to the diversification of the data by including other regions in training. Although the performance is not perfect, this method would be useful when trying to assess susceptibility in places without landslide inventories.

Future research could build on this work by testing in a variety of other regions as well as systematic sensitivity testing for DSM resolution. There should also be more cross-validation of relationships to better understand in what circumstances one relationship can be used to predict susceptibility in another. This method performs best with high-quality landslide inventories at regional scales and can be used as a preliminary analysis to identify areas of greater concern. This method uses globally available data, is easy to implement and adjust, and avoids overfitting relationships to a specific region. This study is a first step in finding a generalizable method that allows the transfer of susceptibility relationships between regions.

Acknowledgements. Computational resources and support from the University of Montana’s Griz Shared Computing Cluster (GSCC) contributed to this research (National Science Foundation Grant No. 1925267). Support for this work was provided by the National Science Foundation Division of Graduate Education under Grant No. 1633831.

5. References

- Adition, A., Kubota, T., & Shinohara, Y. (2018). Comparison of GIS-based landslide susceptibility models using frequency ratio, logistic regression, and artificial neural network in a tertiary region of Ambon, Indonesia. *Geomorphology*, *318*, 101–111. <https://doi.org/10.1016/j.geomorph.2018.06.006>
- Aleotti, P., & Chowdhury, R. (1999). Landslide hazard assessment: Summary review and new perspectives. *Bulletin of Engineering Geology and the Environment*, *58*(1), 21–44. <https://doi.org/10.1007/s100640050066>
- Anbalagan, R., & Singh, B. (1996). Landslide hazard and risk assessment mapping of mountainous terrains - a case study from Kumaun Himalaya, India. *Engineering Geology*, *43*(4), 237–246. [https://doi.org/10.1016/S0013-7952\(96\)00033-6](https://doi.org/10.1016/S0013-7952(96)00033-6)
- Ayalew, L., & Yamagishi, H. (2005). The application of GIS-based logistic regression for landslide susceptibility mapping in the Kakuda-Yahiko Mountains, Central Japan. *Geomorphology*, *65*, 15–31. <https://doi.org/10.1016/j.geomorph.2004.06.010>
- Ayalew, L., Yamagishi, H., & Ugawa, N. (2004). Landslide susceptibility mapping using GIS-based weighted linear combination, the case in Tsugawa area of Agano River, Niigata Prefecture, Japan. *Landslides*, *1*(1), 73–81. <https://doi.org/10.1007/s10346-003-0006-9>
- Baeza, C., & Corominas, J. (2001). Assessment of shallow landslide susceptibility by means of multivariate statistical techniques. *Earth Surface Processes and Landforms*, *26*, 1251–1263. <https://doi.org/10.1002/esp.263>
- Berti, M., Corsini, A., & Daehne, A. (2013). Comparative analysis of surface roughness algorithms for the identification of active landslides. *Geomorphology*, *182*, 1–18. <https://doi.org/10.1016/j.geomorph.2012.10.022>
- Brabb, E. E., Colgan, J. P., & Best, T. C. (1999). Map Showing Inventory and Regional Susceptibility for Holocene Debris Flows, and Related Fast-Moving Landslides in the Conterminous United States: U.S. Geological Survey Miscellaneous Field Studies Map 2329, 2329. Retrieved from <https://pubs.usgs.gov/mf/1999/2329/>
- Budimir, M. E. A., Atkinson, P. M., & Lewis, H. G. (2015). A systematic review of landslide probability mapping using logistic regression. *Landslides*, *12*, 419–436. <https://doi.org/10.1007/s10346-014-0550-5>
- Carrara, A., & Merenda, L. (1976). Landslide inventory in northern Calabria, southern Italy. *Bulletin of the Geological Society of America*, *87*(8), 1153–1162. [https://doi.org/10.1130/0016-7606\(1976\)87<1153:LIINCS>2.0.CO;2](https://doi.org/10.1130/0016-7606(1976)87<1153:LIINCS>2.0.CO;2)
- Carrara, Alberto. (1983). Multivariate Models for Landslide Hazard Evaluation. *Mathematical Geology*, *15*(3), 403–426. <https://doi.org/10.1007/BF01031290>
- Chowdhury, R. N., & Zhang, S. (1993). Modelling the risk of progressive slope failure: A new approach. *Reliability Engineering and System Safety*, *40*, 17–30. [https://doi.org/10.1016/0951-8320\(93\)90115-F](https://doi.org/10.1016/0951-8320(93)90115-F)
- Conoscenti, C., Rotigliano, E., Cama, M., Caraballo-Arias, N. A., Lombardo, L., & Agnesi, V. (2016). Exploring the effect of absence selection on landslide susceptibility models: A case study in Sicily, Italy. *Geomorphology*, *261*, 222–235. <https://doi.org/10.1016/j.geomorph.2016.03.006>
- Craney, T. A., & Surlis, J. G. (2002). Model-Dependent Variance Inflation Factor Cutoff Values. *Quality Engineering*, *14*(3), 391–403. <https://doi.org/10.1081/QEN-120001878>
- Crawford, M. M. (2021). Kentucky Geological Survey landslide inventory [2021-01]: Kentucky

- Geological Survey Research Data. <https://doi.org/doi.org/10.13023/kgs.data.2021.02>
- Dehnavi, A., Aghdam, I. N., Pradhan, B., & Morshed Varzandeh, M. H. (2015). A new hybrid model using step-wise weight assessment ratio analysis (SWARA) technique and adaptive neuro-fuzzy inference system (ANFIS) for regional landslide hazard assessment in Iran. *Catena*, *135*, 122–148. <https://doi.org/10.1016/j.catena.2015.07.020>
- Domínguez-Cuesta, M. J., Jiménez-Sánchez, M., & Berrezueta, E. (2007). Landslides in the Central Coalfield (Cantabrian Mountains, NW Spain): Geomorphological features, conditioning factors and methodological implications in susceptibility assessment. *Geomorphology*, *89*(3–4), 358–369. <https://doi.org/10.1016/j.geomorph.2007.01.004>
- Van Den Eeckhaut, M., Poesen, J., Verstraeten, G., Vanacker, V., Nyssen, J., Moeyersons, J., et al. (2007). Use of LIDAR-derived images for mapping old landslides under forest. *Earth Surface Processes and Landforms*, *32*, 754–769. <https://doi.org/10.1002/esp.1417>
- Farrar, D. E., & Glauber, R. R. (1967). Multicollinearity in Regression Analysis: The Problem Revisited. *The Review of Economic and Statistics*, *49*(1), 92–107. Retrieved from <https://www.jstor.org/stable/1937887>
- Feizizadeh, B., & Blaschke, T. (2014). An uncertainty and sensitivity analysis approach for GIS-based multicriteria landslide susceptibility mapping. *International Journal of Geographical Information Science*, *28*(3), 610–638. <https://doi.org/10.1080/13658816.2013.869821>
- Fiorucci, F., Ardizzone, F., Mondini, A. C., Viero, A., & Guzzetti, F. (2019). Visual interpretation of stereoscopic NDVI satellite images to map rainfall-induced landslides. *Landslides*, *16*(1), 165–174. <https://doi.org/10.1007/s10346-018-1069-y>
- Günther, A., Van Den Eeckhaut, M., Malet, J. P., Reichenbach, P., & Hervás, J. (2014). Climate-physiographically differentiated Pan-European landslide susceptibility assessment using spatial multi-criteria evaluation and transnational landslide information. *Geomorphology*, *224*, 69–85. <https://doi.org/10.1016/j.geomorph.2014.07.011>
- Guzzetti, F., Carrara, A., Cardinali, M., & Reichenbach, P. (1999). Landslide hazard evaluation: a review of current techniques and their application in a multi-scale study, Central Italy. *Geomorphology*, *31*, 181–216.
- Guzzetti, F., Reichenbach, P., Ardizzone, F., Cardinali, M., & Galli, M. (2006). Estimating the quality of landslide susceptibility models. *Geomorphology*, *81*(1–2), 166–184. <https://doi.org/10.1016/j.geomorph.2006.04.007>
- Guzzetti, F., Galli, M., Reichenbach, P., Ardizzone, F., & Cardinali, M. (2006). Landslide hazard assessment in the Collazzone area, Umbria, central Italy. *Natural Hazards and Earth System Science*, *6*(1), 115–131. <https://doi.org/10.5194/nhess-6-115-2006>
- Hadji, R., Boumazbeur, A. errahmane, Limani, Y., Baghem, M., Chouabi, A. el M., & Demdoum, A. (2013). Geologic, topographic and climatic controls in landslide hazard assessment using GIS modeling: A case study of Souk Ahras region, NE Algeria. *Quaternary International*, *302*, 224–237. <https://doi.org/10.1016/j.quaint.2012.11.027>
- Haiden, T., & Pistotnik, G. (2009). Intensity-dependent parameterization of elevation effects in precipitation analysis. *Advances in Geosciences*, *20*, 33–38. <https://doi.org/10.5194/adgeo-20-33-2009>
- Hong, H., Pourghasemi, H. R., & Pourtaghi, Z. S. (2016). Landslide susceptibility assessment in Lianhua County (China): A comparison between a random forest data mining technique and bivariate and multivariate statistical models. *Geomorphology*, *259*, 105–118. <https://doi.org/10.1016/j.geomorph.2016.02.012>
- Hong, H., Liu, J., Bui, D. T., Pradhan, B., Acharya, T. D., Pham, B. T., et al. (2018). Landslide

- susceptibility mapping using J48 Decision Tree with AdaBoost, Bagging and Rotation Forest ensembles in the Guangchang area (China). *Catena*, 163, 399–413.
<https://doi.org/10.1016/j.catena.2018.01.005>
- Hong, Y., Adler, R., & Huffman, G. (2007). Use of satellite remote sensing data in the mapping of global landslide susceptibility. *Natural Hazards*, 43, 245–256.
<https://doi.org/10.1007/s11069-006-9104-z>
- Hosmer, D. W., & Lemeshow, S. (2000). Applied Logistic Regression, Wiley Series in Probability and Statistics, Wiley Series in Probability and Statistics: Texts and References Section.
- Jenness, J., Brost, B., & Beier, P. (2013). Manual: Land Facet Corridor Designer. *Jenness Enterprises*, (January). Retrieved from http://www.jennessent.com/arcgis/land_facets.htm
- Jones, E. S., Mirus, B. B., Schmitt, R. G., Baum, R. L., Burns, W. J., Crawford, M., et al. (2019). Summary Metadata – Landslide Inventories across the United States. *U.S. Geological Survey Data Release*. <https://doi.org/https://doi.org/10.5066/P9E2A37P>.
- Kienholz, H. (1978). Maps of Geomorphology and Natural Hazards of Grindelwald, Switzerland: Scale 1:10,000. *Arctic and Alpine Research*, 10(2), 168.
<https://doi.org/10.2307/1550751>
- Kirschbaum, D., Stanley, T., & Yatheendradas, S. (2016). Modeling landslide susceptibility over large regions with fuzzy overlay. *Landslides*, 13(3), 485–496.
<https://doi.org/10.1007/s10346-015-0577-2>
- Kornejady, A., Ownegh, M., & Bahremand, A. (2017). Landslide susceptibility assessment using maximum entropy model with two different data sampling methods. *Catena*, 152, 144–162.
<https://doi.org/10.1016/j.catena.2017.01.010>
- Kritikos, T., Robinson, T. R., & Davie, T. R. H. (2015). Regional coseismic landslide hazard assessment without historical landslide inventories: A new approach. *Journal of Geophysical Research: Earth Surface*, 120, 711–729.
<https://doi.org/10.1002/2014JF003224>
- Larsen, M. C., & Torres-Sanchez, A. J. (1998). The frequency and distribution of recent landslides in three montane tropical regions of Puerto Rico. *Geomorphology*, (24), 309–331.
- Lee, S. (2005). Application and cross-validation of spatial logistic multiple regression for landslide susceptibility analysis. *Geosciences Journal*, 9(1), 63–71.
<https://doi.org/10.1007/BF02910555>
- Lombardo, L., Cama, M., Maerker, M., & Rotigliano, E. (2014). A test of transferability for landslides susceptibility models under extreme climatic events: application to the Messina 2009 disaster. *Natural Hazards*, 74, 1951–1989. <https://doi.org/10.1007/s11069-014-1285-2>
- Martz, L. W. (1992). The variation of soil erodibility with slope position in a cultivated canadian prairie landscape. *Earth Surface Processes and Landforms*, 17(6), 543–556.
<https://doi.org/10.1002/esp.3290170602>
- Moore, I. D., Grayson, R. B., & Ladson, A. R. (1991). Digital Terrain Modelling: A review of Hydrological, Geomorphological, and Biological Applications. *Hydrological Processes*, 5, 3–30. <https://doi.org/10.1002/hyp.3360050103>
- Naranjo, J. L., Van Westen, C. J., & Soeters, R. (1994). Evaluating the use of training areas in bivariate statistical landslide hazard analysis - a case study in Colombia. *ITC Journal*.
- Neuland, H. (1976). A Prediction Model of Landslips. *Catena*, 3, 215–230.
- Nilsen, T. H., Wright, R. H., Vlastic, T. C., & Spangle, W. E. (1979). Relative slope stability and land-use planning in the San Francisco Bay region, California. *US Geological Survey*

- Professional Paper, 944, 96.*
- North Carolina Geological Survey (2021). NCGS Landslide Read Deposit Polygons. Retrieved from <https://www.nconemap.gov/datasets/ncdenr::ncgs-landslide-read-deposit-polygons/about>
- Peirce, C. S. (1884). The numerical measure of the success of predicitions. *Science*, 4(93), 453–454.
- Pelletier, J. D., Barron-Gafford, G. A., Breshears, D. D., Brooks, P. D., Chorover, J., Durcik, M., et al. (2013). Coevolution of nonlinear trends in vegetation, soils, and topography with elevation and slope aspect: A case study in the sky islands of southern Arizona. *Journal of Geophysical Research: Earth Surface*, 118, 741–758. <https://doi.org/10.1002/jgrf.20046>
- Pham, B. T., Shirzadi, A., Shahabi, H., Omidvar, E., Singh, S. K., Sahana, M., et al. (2019). Landslide susceptibility assessment by novel hybrid machine learning algorithms. *Sustainability (Switzerland)*, 11(16), 1–25. <https://doi.org/10.3390/su11164386>
- QGIS Development Team. (2009). QGIS Geographic Information System. *Open Source Geospatial Foundation*. Retrieved from <http://qgis.osgeo.org>
- R Core Team. (2020). R: A Language and environment for statistical computing. Vienna, Austria: R Foundation for Statistical Computing. Retrieved from <https://www.r-project.org/>
- Radbruch-Hall, D. H., & Varnes, D. J. (1976). Landslides - Cause and Effect. *Bulletin of the International Association of Engineering Geology*, 14, 205–216. <https://doi.org/10.1007/BF02634797>
- Ray, R. L., & Jacobs, J. M. (2007). Relationships among remotely sensed soil moisture, precipitation and landslide events. *Natural Hazards*, 43, 211–222. <https://doi.org/10.1007/s11069-006-9095-9>
- Reichenbach, P., Rossi, M., Malamud, B. D., Mihir, M., & Guzzetti, F. (2018). A review of statistically-based landslide susceptibility models. *Earth-Science Reviews*, 180(March), 60–91. <https://doi.org/10.1016/j.earscirev.2018.03.001>
- Roering, J. J., Kirchner, J. W., & Dietrich, W. E. (2001). Hillslope evolution by nonlinear, slope-dependent transport: Steady state morphology and equilibrium adjustment timescales. *Journal of Geophysical Research: Solid Earth*, 106(B8), 16499–16513. <https://doi.org/10.1029/2001jb000323>
- Von Ruetten, J., Papritz, A., Lehmann, P., Rickli, C., & Or, D. (2011). Spatial statistical modeling of shallow landslides-Validating predictions for different landslide inventories and rainfall events. *Geomorphology*, 133(1–2), 11–22. <https://doi.org/10.1016/j.geomorph.2011.06.010>
- Schuster, R. L., & Highland, L. M. (2001). Socioeconomic and Environmental Impacts of Landslides in the Western Hemisphere. *U.S. Geological Survey Open-File Report*. Retrieved from <http://pubs.usgs.gov/of/2001/ofr-01-0276/>
- Shahabi, H., Khezri, S., Ahmad, B. Bin, & Hashim, M. (2014). Landslide susceptibility mapping at central Zab basin, Iran: A comparison between analytical hierarchy process, frequency ratio and logistic regression models. *Catena*, 115, 55–70. <https://doi.org/10.1016/j.catena.2013.11.014>
- Shirzadi, A., Solaimani, K., Roshan, M. H., Kaviani, A., Chapi, K., Shahabi, H., et al. (2019). Uncertainties of prediction accuracy in shallow landslide modeling: Sample size and raster resolution. *Catena*, 178, 172–188. <https://doi.org/10.1016/j.catena.2019.03.017>
- Soeters, R. S., & Van Westen, C. J. (1996). Slope instability recognition, analysis, and zonation. In: Turner, A. K., Schuster, R. L. (eds) Landslides: investigation and mitigation. Special Report. *Transportation Research Board, National Research Council*, 247, 129–173.

- Speight, J. G. (1980). The Role of Topography in Controlling Throughflow Generation: a Discussion. *Earth Surface Processes*, 5, 187–191. <https://doi.org/10.1002/esp.3760050209>
- Stanley, T., & Kirschbaum, D. B. (2017). A heuristic approach to global landslide susceptibility mapping. *Natural Hazards*, 87(1), 145–164. <https://doi.org/10.1007/s11069-017-2757-y>
- Stephenson, D. B. (2000). Use of the “Odds Ratio” for Diagnosing Forecast Kill. *Weather and Forecasting*, 15(2), 221–232. [https://doi.org/10.1175/1520-0434\(2000\)015<0221:UOTORF>2.0.CO;2](https://doi.org/10.1175/1520-0434(2000)015<0221:UOTORF>2.0.CO;2)
- Stevenson, P. C. (1977). An empirical method for the evaluation of relative landslide risk. *Bulletin of the International Association of Engineering Geology*, 16(1), 69–72. <https://doi.org/10.1007/BF02591451>
- Swets, J. A. (1988). Measuring the Accuracy of Diagnostic Systems. *Science*, 240(4857), 1285–1293.
- Takaku, J., Tadono, T., & Tsutsui, K. (2014). Generation of high resolution global DSM from ALOS PRISM. *International Archives of the Photogrammetry, Remote Sensing and Spatial Information Sciences - ISPRS Archives*, 40(4), 243–248. <https://doi.org/10.5194/isprsarchives-XL-4-243-2014>
- Tsui, C.-C., Chen, Z.-S., & Hsieh, C.-F. (2004). Relationships between soil properties and slope position in a lowland rain forest of southern Taiwan. *Geoderma*, 123, 131–142. <https://doi.org/10.1016/j.geoderma.2004.01.031>
- USGS. (2019). How many deaths result from landslides each year? Retrieved from https://www.usgs.gov/faqs/how-many-deaths-result-landslides-each-year?qt-news_science_products=0#qt-news_science_products
- Utah Geological Survey (2016). Landslide Inventory Polygons. Retrieved from <https://gis.utah.gov/data/geoscience/landslides/>
- Weiss, A. D. (2000). Topographic position and landforms analysis. *Poster Presentation, ESRI User Conference, San Diego, CA*. Retrieved from <http://scholar.google.com/scholar?hl=en&btnG=Search&q=intitle:Topographic+Position+and+Landforms+Analysis#0>
- van Westen, C. J., van Asch, T. W. J., & Soeters, R. (2006). Landslide hazard and risk zonation - Why is it still so difficult? *Bulletin of Engineering Geology and the Environment*, 65, 167–184. <https://doi.org/10.1007/s10064-005-0023-0>
- Washington Geological Survey (2020). *Landslide protocol inventory mapping-- GIS data, February, 2020: Washington Geological Survey Digital Data Series 19, version 2.0, previously released January, 2019*. Retrieved from https://fortress.wa.gov/dnr/geologydata/publications/data_download/ger_portal_landslide_inventory.zip
- Wu, T. H., & Kraft, L. M. (1970). Safety Analysis of Slopes. *Journal of the Soil Mechanics and Foundations Division*, 96(2), 609–630. <https://doi.org/10.1061/JSFEAQ.0001406>
- Yalcin, A., Reis, S., Aydinoglu, A. C., & Yomralioglu, T. (2011). A GIS-based comparative study of frequency ratio, analytical hierarchy process, bivariate statistics and logistics regression methods for landslide susceptibility mapping in Trabzon, NE Turkey. *Catena*, 85(3), 274–287. <https://doi.org/10.1016/j.catena.2011.01.014>
- Youssef, Ahmed M., Pradhan, B., Jebur, M. N., & El-Harbi, H. M. (2015). Landslide susceptibility mapping using ensemble bivariate and multivariate statistical models in Fayfa area, Saudi Arabia. *Environmental Earth Sciences*, 73(7), 3745–3761. <https://doi.org/10.1007/s12665-014-3661-3>

- Youssef, Ahmed Mohamed, Pourghasemi, H. R., Pourtaghi, Z. S., & Al-Katheeri, M. M. (2016). Landslide susceptibility mapping using random forest, boosted regression tree, classification and regression tree, and general linear models and comparison of their performance at Wadi Tayyah Basin, Asir Region, Saudi Arabia. *Landslides*, *13*, 839–856. <https://doi.org/10.1007/s10346-015-0614-1>
- Yule, G. U. (1900). On the association of attributes in statistics. *Philosophical Transactions of the Royal Society of London*, *194(A)*, 257–319.

6 Supplementary Information

Table S1. % LS represents the percentage of landslides classified in “high” – “very high” susceptibility classes. % area represents the percentage of area classified as “high” – “very high” susceptibility for each region. Three methods were used to classify data into susceptibility classes: Jenks natural breaks, equal intervals ranging from minimum to maximum susceptibility, and equal intervals ranging from 0 to 1.

Region	Logistic Regression						Frequency Ratio					
	High - Very High						High - Very High					
	Jenks		Equal (min - max)		Equal (0 - 1)		Jenks		Equal (min - max)		Equal (0 - 1)	
	% LS	% area	% LS	% area	% LS	% area	% LS	% area	% LS	% area	% LS	% area
wa1sf	0.846	0.333	0.846	0.333	0.778	0.280	0.930	0.313	0.797	0.435	1.000	0.985
wa2sf	0.719	0.253	0.828	0.171	0.705	0.164	0.864	0.292	0.843	0.313	0.966	0.589
wa3sf	0.768	0.300	0.764	0.303	0.718	0.267	0.947	0.472	0.917	0.521	0.995	0.740
wa4sf	0.681	0.307	0.681	0.307	0.588	0.224	0.882	0.320	0.685	0.544	1.000	0.967
ut1s	0.761	0.200	0.811	0.143	0.753	0.137	0.861	0.280	0.857	0.288	0.990	0.764
nc1sm	0.623	0.412	0.739	0.336	0.618	0.218	0.566	0.484	0.764	0.409	0.994	1.000
wa1d	0.790	0.386	0.698	0.485	0.479	0.204	0.957	0.316	0.599	0.703	1.000	1.000
wa2d	0.706	0.242	0.717	0.234	0.663	0.213	0.876	0.302	0.763	0.440	0.990	0.859
wa3d	0.707	0.498	0.764	0.442	0.555	0.310	0.883	0.474	0.730	0.636	0.999	0.975
wa4d	0.745	0.553	0.788	0.507	0.428	0.242	0.904	0.527	0.758	0.718	1.000	1.000
ut1d	0.748	0.448	0.676	0.521	0.493	0.302	0.934	0.467	0.693	0.768	1.000	1.000
nc1d	0.673	0.454	0.697	0.286	0.455	0.210	0.830	0.543	0.704	0.511	1.000	1.000
wa1	0.755	0.425	0.709	0.460	0.573	0.327	0.783	0.402	0.677	0.492	1.000	1.000
wa2	0.707	0.252	0.733	0.234	0.670	0.215	0.874	0.289	0.758	0.412	0.989	0.847
wa3	0.735	0.474	0.753	0.458	0.600	0.345	0.896	0.457	0.726	0.643	0.999	0.974
wa4	0.701	0.420	0.640	0.482	0.392	0.232	0.918	0.415	0.621	0.750	1.000	0.997
ut1	0.713	0.453	0.664	0.502	0.454	0.286	0.865	0.449	0.658	0.685	1.000	1.000
nc1	0.673	0.230	0.694	0.197	0.450	0.193	0.810	0.218	0.758	0.218	1.000	0.903
ky1	0.777	0.273	0.575	0.180	0.202	0.177	0.668	0.327	0.679	0.172	1.000	0.943
ky1a	0.497	0.407	0.713	0.382	0.240	0.196	0.516	0.432	0.667	0.595	1.000	1.000
ky2	0.717	0.413	0.796	0.389	0.548	0.198	0.774	0.499	0.835	0.578	1.000	1.000
ky21	0.662	0.584	0.817	0.391	0.567	0.118	0.846	0.487	0.864	0.498	1.000	1.000
ky31	0.736	0.509	0.772	0.309	0.729	0.132	0.756	0.466	0.756	0.337	0.990	1.000

Table S2. Variance inflation factors (VIF) for each classified variable. VIF values less than 5 do not exhibit problematic multicollinearity.

	elevation class	slope class	aspect class	plan class	profile class	tpi class
ky3	1.124	1.110	1.010	1.271	1.311	1.223
ky3a	1.128	1.113	1.009	1.260	1.300	1.221
ky4	1.310	1.127	1.016	1.245	1.314	1.362
ky4l	1.314	1.112	1.032	1.224	1.287	1.346
ky5l	1.164	1.169	1.072	1.326	1.396	1.275
nc1	1.116	1.153	1.014	1.340	1.345	1.258
nc1sm	1.250	1.230	1.050	1.306	1.315	1.262
nc1d	1.114	1.151	1.014	1.340	1.341	1.263
ut1	1.081	1.128	1.020	1.301	1.343	1.290
ut1s	1.218	1.221	1.076	1.252	1.361	1.330
ut1d	1.070	1.105	1.021	1.308	1.346	1.273
wa1sf	1.168	1.221	1.059	1.260	1.312	1.222
wa2sf	1.194	1.227	1.038	1.349	1.387	1.239
wa3sf	1.089	1.117	1.022	1.254	1.253	1.123
wa4sf	1.052	1.087	1.046	1.291	1.317	1.239
wa1d	1.102	1.176	1.010	1.329	1.350	1.237
wa2d	1.089	1.110	1.045	1.393	1.436	1.248
wa3d	1.193	1.256	1.011	1.319	1.309	1.145
wa4d	1.076	1.103	1.025	1.316	1.338	1.259
wa1	1.173	1.247	1.013	1.319	1.349	1.239
wa2	1.095	1.112	1.044	1.400	1.445	1.240
wa3	1.192	1.252	1.011	1.316	1.307	1.142
wa4	1.073	1.102	1.024	1.316	1.349	1.256

Table S3. Logistic regression model coefficients.

	ky1	ky1a	ky2	ky21	ky31	nc1	nc1d	nc1sm	ut1	ut1d
tpi_class5	-0.433	-0.365	-1.307	-1.577	-0.033	-0.917	-0.877	-1.396	-0.385	-0.393
tpi_class4	-0.19	-0.131	-0.673	-0.825	-0.36	-0.776	-0.723	-1.421	-0.193	-0.189
tpi_class3	-0.02	0.011	-0.238	-0.414	-0.083	-0.421	-0.385	-1.095	-0.239	-0.216
tpi_class2	0.043	0.061	0.025	-0.015	0.016	-0.153	-0.127	-0.562	0.017	0.029
profile_classupwardly convex	-0.137	-0.117	-0.247	0.048	-0.285	0.04	0.095	0.016	0.228	0.198
profile_classupwardly concave	-0.009	-0.008	-0.165	0.133	-0.275	-0.009	0.046	0.154	0.2	0.171
plan_classlaterally convex	-0.157	-0.157	-0.159	-0.236	0.233	0.145	0.115	0.037	0.207	0.207
plan_classlaterally concave	0.075	0.032	0.139	0.238	0.209	0.302	0.273	0.21	0.24	0.25
aspect_classW	0.083	0.096	-0.242	-0.149	0.255	-0.199	-0.171	-1.24	0.046	0.012
aspect_classS	0.105	0.087	-0.302	-0.323	0.781	-0.162	-0.164	-0.281	0.156	0.136
aspect_classN	0.106	0.058	-0.036	0.246	-0.153	0.331	0.365	-0.879	0.441	0.426
slope_class40-50 deg	1.615	0.653	9.822	10.347	-0.064	0.129	-0.672	2.867	0.33	-0.137
slope_class30-40 deg	1.21	0.329	9.842	10.52	15.011	-0.183	-0.496	0.683	0.241	1.129
slope_class20-30 deg	0.844	-0.058	9.588	10.809	15.116	0.21	-0.045	0.275	1.038	2.526
slope_class10-20 deg	0.66	-0.297	9.693	10.978	13.515	0.943	0.745	-0.375	1.552	3.128
slope_class0-10 deg	0.095	-0.787	9.575	9.993	11.76	0.851	0.658	-1.748	1.346	2.933
elevation_class7	-11.23	-11.55	-7.78	-8.795	0.631	-2.283	-2.498	-3.663	2.517	2.208
elevation_class6	-2.322	-2.825	3.574	4.058	14.643	-1.584	-1.576	-3.649	2.834	2.736
elevation_class5	-2.288	-2.542	3.663	3.82	15.652	-1.382	-1.331	-3.23	2.852	2.76
elevation_class4	0.674	0.633	2.691	2.882	16.512	-0.413	-0.337	-2.681	1.954	1.872
elevation_class3	0.018	-0.189	1.661	2.051	17.111	0.307	0.392	-1.667	1.963	1.96
elevation_class2	0.002	-0.111	1.102	0.908	16.787	-0.46	-0.415	-1.717	1.018	0.915
(Intercept)	-0.673	0.371	-11.571	-13.176	-29.388	-0.393	-0.319	3.064	-4.053	-5.479

utls	wal	wald	walsf	wa2	wa2d	wa2sf	wa3	wa3d	wa3sf	wa4	wa4d	wa4sf
-0.21	-0.12	-0.118	0.413	0.035	-0.216	1.322	-0.167	-0.233	0.358	-0.259	-0.282	-0.034
-0.728	-0.087	-0.088	0.303	-0.137	-0.252	0.786	-0.193	-0.229	0.107	-0.24	-0.22	-0.262
-0.761	-0.255	-0.222	-0.09	-0.498	-0.585	0.115	-0.313	-0.324	-0.144	-0.227	-0.306	-0.186
-0.481	-0.013	0.043	0.037	-0.252	-0.318	0.072	-0.071	-0.094	-0.021	-0.055	-0.081	-0.135
0.388	0.404	0.342	0.246	0.662	0.728	0.593	0.361	0.362	0.232	0.25	0.402	0.396
0.443	0.479	0.402	0.435	0.84	0.857	1.007	0.395	0.385	0.318	0.296	0.432	0.405
-0.028	0.47	0.666	0.148	0.712	0.705	0.785	0.355	0.391	0.299	0.146	0.156	0.178
0.137	0.559	0.716	0.291	0.858	0.83	0.976	0.414	0.449	0.326	0.22	0.242	0.154
0.455	-0.151	-0.014	-0.295	0.107	0.15	-0.162	0.483	0.499	0.338	-0.582	-0.565	-0.633
0.347	-0.011	0.044	0.002	0.02	0.003	-0.012	0.485	0.464	0.537	-0.154	-0.183	-0.062
0.8	0.031	0.279	-0.149	0.199	0.246	0.041	0.199	0.198	0.246	-0.075	-0.099	-0.249
0.11	0.26	0.178	-0.466	-0.438	-0.104	-1.354	0.128	0.459	-0.304	0.005	0.376	-0.619
-0.852	0.245	0.445	-0.641	-0.439	-0.233	-1.577	0.269	0.789	-0.672	0.058	0.778	-0.771
-1.96	0.626	1.091	-0.706	-0.785	-0.379	-2.215	0.621	1.26	-1.034	0.433	1.339	-0.942
-3.304	0.685	1.519	-1.712	-1.305	-0.823	-3.312	0.523	1.224	-1.887	0.643	1.749	-1.796
-5.334	-0.237	0.618	-3.913	-2.802	-2.283	-5.082	-0.358	0.34	-3.083	0.08	1.235	-2.727
5.203	-15.77	-17.79	-18.16	0.066	-0.012	-0.005	-9.817	-9.49	-10.25	1.303	0.942	2.705
4.027	-15.77	-17.61	-18.29	0.35	0.519	0.406	-0.555	-1.199	1.777	2.141	1.587	3.838
4.189	-15.876	-18.029	-17.855	0.544	0.102	1.127	1.185	1.08	2.064	3.062	2.889	3.687
3.609	-4.868	-18.06	-17.712	0.901	0.915	0.311	1.416	1.341	1.785	2.692	2.539	3.441
2.067	-1.938	-17.983	-8.353	0.75	0.803	-0.962	1.035	0.956	1.724	2.663	2.636	2.669
2.72	0.139	-0.713	-0.681	-1.084	-1.191	-0.618	1.166	1.102	1.587	1.955	1.89	2.275
-1.733	-0.9	-1.514	1.686	0.714	0.332	1.772	-1.911	-2.52	-0.767	-2.996	-4.017	-1.973

Table S4. Frequency Ratio values

	kv1	kv1a	kv2	kv21	kv31	nc1	nc1d	nc1sm	ut1	ut1d	ut1s
tpi 5	0.860	0.880	0.703	0.624	1.090	0.700	0.703	0.848	0.828	0.828	1.356
tpi 4	0.966	0.978	0.969	0.939	0.828	0.785	0.792	0.773	1.008	1.008	0.912
tpi 3	1.023	1.023	1.089	1.053	0.950	0.997	0.999	0.847	1.004	1.004	0.741
tpi 2	1.054	1.048	1.081	1.166	1.084	1.149	1.148	1.122	1.108	1.108	1.001
tpi 1	1.038	1.021	0.948	1.038	1.129	1.210	1.196	1.397	0.999	0.999	1.345
profile flat	0.980	0.989	1.146	1.017	0.784	0.995	0.971	0.782	0.894	0.894	0.484
profile upwardly convex	0.996	0.996	0.959	0.988	1.051	1.078	1.077	1.056	1.024	1.024	1.014
profile upwardly concave	1.005	1.004	1.032	1.011	0.961	0.905	0.908	0.945	0.982	0.982	1.010
plan flat	0.942	0.965	1.002	0.842	0.640	0.936	0.945	0.748	0.907	0.907	0.590
plan laterally concave	1.060	1.047	1.101	1.147	1.033	1.093	1.091	1.092	1.034	1.034	1.053
plan laterally convex	0.940	0.953	0.886	0.831	1.006	0.902	0.903	0.909	0.977	0.977	0.985
aspect W	1.013	1.024	0.969	0.965	0.922	0.906	0.911	0.616	0.924	0.924	0.988
aspect S	1.002	0.997	0.924	0.893	1.247	0.916	0.908	1.154	0.992	0.992	1.076
aspect E	0.967	0.974	1.055	1.004	0.824	0.993	0.987	1.187	0.949	0.949	0.789
aspect N	1.019	1.003	1.049	1.124	0.920	1.158	1.164	0.842	1.131	1.131	1.100
slope >50 deg	0.667	1.000	0.000	0.000	0.000	0.636	0.696	0.669	0.088	0.088	1.789
slope 40-50 deg	1.355	1.344	0.641	0.334	0.000	0.603	0.404	1.832	0.089	0.089	1.868
slope 30-40 deg	1.200	1.218	0.811	0.726	1.789	0.516	0.480	1.292	0.281	0.281	1.689
slope 20-30 deg	1.064	1.064	0.950	1.029	1.831	0.737	0.720	1.186	0.794	0.794	1.253
slope 10-20 deg	0.997	0.974	1.065	1.144	1.347	1.139	1.144	1.016	1.137	1.137	0.610
slope 0-10 deg	0.749	0.775	0.993	0.633	0.418	1.086	1.091	0.458	1.054	1.054	0.110
elevation 7	0.000	0.000	0.000	0.000	0.000	0.162	0.125	0.321	0.960	0.960	1.677
elevation 6	0.174	0.126	1.288	1.256	0.122	0.300	0.282	0.398	1.226	1.226	1.223
elevation 5	0.179	0.166	1.426	1.393	0.558	0.369	0.361	0.554	1.289	1.289	0.907
elevation 4	1.228	1.272	1.049	1.061	1.261	0.811	0.813	0.709	0.823	0.823	0.746
elevation 3	0.962	0.926	0.583	0.693	1.492	1.234	1.243	0.973	0.766	0.766	0.454
elevation 2	0.976	0.990	0.409	0.296	0.958	0.881	0.874	0.914	0.414	0.414	0.675
elevation 1	0.911	0.984	0.159	0.090	0.000	1.100	1.073	1.601	0.205	0.205	0.032

wal	wald	walsf	wa2	wa2d	wa2sf	wa3	wa3d	wa3sf	wa4	wa4d	wa4sf
1.027	0.966	1.275	1.279	1.208	1.479	1.075	1.043	1.273	0.981	0.964	1.084
1.055	1.036	1.107	1.115	1.106	1.191	1.063	1.056	1.094	0.994	1.009	0.977
0.930	0.959	0.843	0.766	0.780	0.698	0.898	0.907	0.827	0.954	0.949	0.940
1.078	1.089	1.009	1.009	1.028	0.843	1.083	1.086	1.007	1.069	1.076	1.002
1.106	1.061	1.098	1.291	1.327	1.069	1.154	1.157	1.130	1.099	1.111	1.118
0.608	0.703	0.441	0.268	0.279	0.180	0.451	0.470	0.384	0.576	0.592	0.465
1.009	1.013	0.972	1.002	1.024	0.897	1.011	1.016	0.975	1.017	1.024	1.004
1.011	1.003	1.050	1.083	1.061	1.168	1.025	1.018	1.056	1.001	0.995	1.018
0.646	0.685	0.521	0.347	0.368	0.256	0.493	0.505	0.368	0.696	0.725	0.556
1.041	1.032	1.030	1.080	1.092	1.032	1.052	1.054	1.030	1.041	1.044	1.022
1.000	1.006	1.018	1.067	1.054	1.117	1.019	1.016	1.042	0.987	0.983	1.015
0.940	0.957	0.930	1.048	1.059	0.988	1.092	1.099	1.060	0.788	0.790	0.788
1.022	0.959	1.020	0.976	0.950	1.036	1.089	1.083	1.091	1.004	0.995	1.025
1.022	0.962	1.065	0.911	0.905	0.951	0.817	0.816	0.798	1.084	1.097	1.071
1.029	1.100	1.006	1.055	1.066	1.041	0.951	0.946	1.005	1.054	1.041	1.035
0.504	0.221	1.187	1.878	1.807	1.978	0.966	0.660	1.724	0.600	0.238	1.671
0.738	0.346	1.230	1.727	1.680	1.876	1.077	0.905	1.630	0.706	0.440	1.317
0.862	0.544	1.296	1.677	1.602	1.789	1.145	1.069	1.488	0.857	0.711	1.343
1.119	0.941	1.365	1.557	1.539	1.644	1.270	1.258	1.297	1.065	1.001	1.292
1.208	1.260	1.004	1.330	1.340	1.217	1.150	1.174	0.789	1.149	1.183	0.828
0.764	0.915	0.248	0.508	0.537	0.350	0.503	0.529	0.180	0.767	0.834	0.329
0.000	0.000	0.000	1.379	1.311	1.619	0.000	0.000	0.000	0.457	0.393	0.618
0.000	0.000	0.000	1.464	1.442	1.707	0.494	0.286	1.400	0.809	0.620	1.298
0.000	0.000	0.000	1.543	1.358	1.778	1.259	1.221	1.474	1.273	1.235	1.351
0.021	0.000	0.000	1.636	1.632	1.589	1.374	1.359	1.345	1.106	1.082	1.186
0.329	0.000	0.002	1.455	1.479	0.880	1.189	1.173	1.258	1.082	1.136	0.697
1.201	0.919	1.143	0.590	0.544	0.826	1.235	1.229	1.165	0.721	0.751	0.525
1.015	1.204	1.086	0.977	0.996	0.916	0.524	0.555	0.242	0.131	0.146	0.056

Figure S1. AUC (area under relative operating characteristics curve) values for different training to testing ratios. S, F, SM = scarps, flanks, individual slope movements; deposits = dominated by deposits data; KY Aerial = dominated by aerial-derived landslides; KY LiDAR = dominated by lidar-derived landslides. 70_30 = 70% training, 30% testing; 80_20 = 80% training, 20% testing; 60_40 = 60% training, 40% testing.

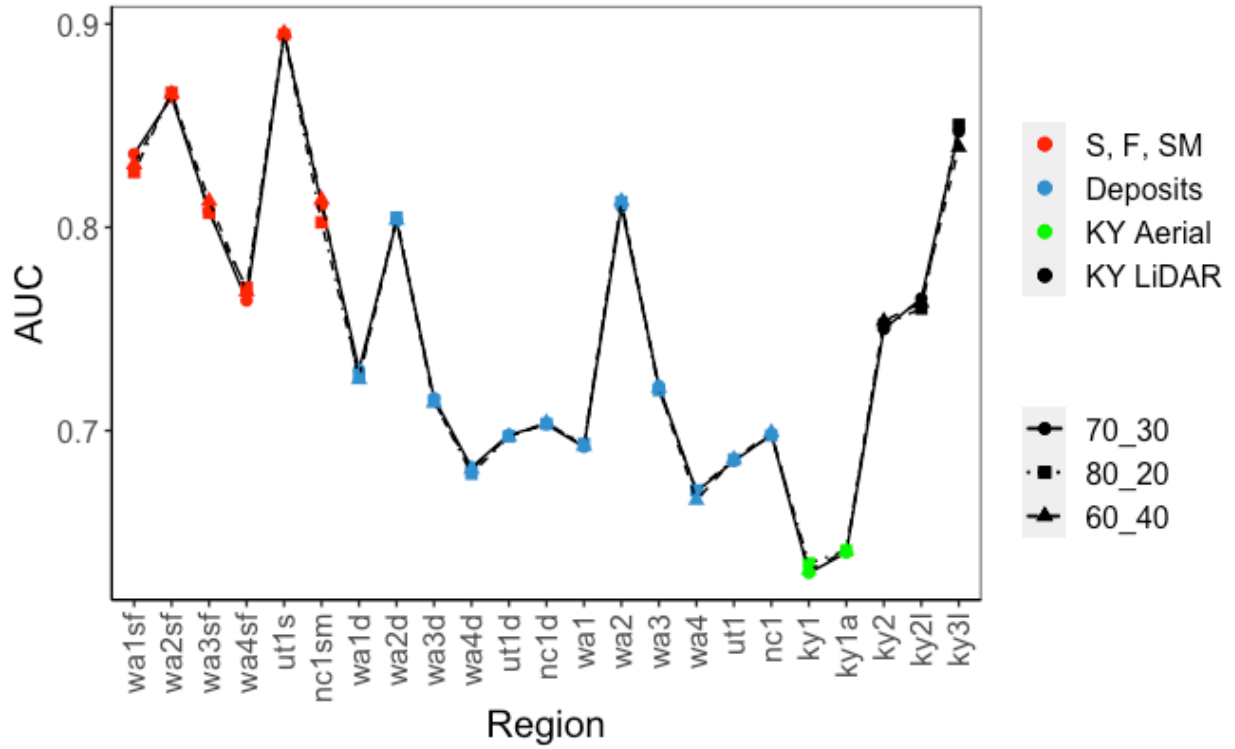
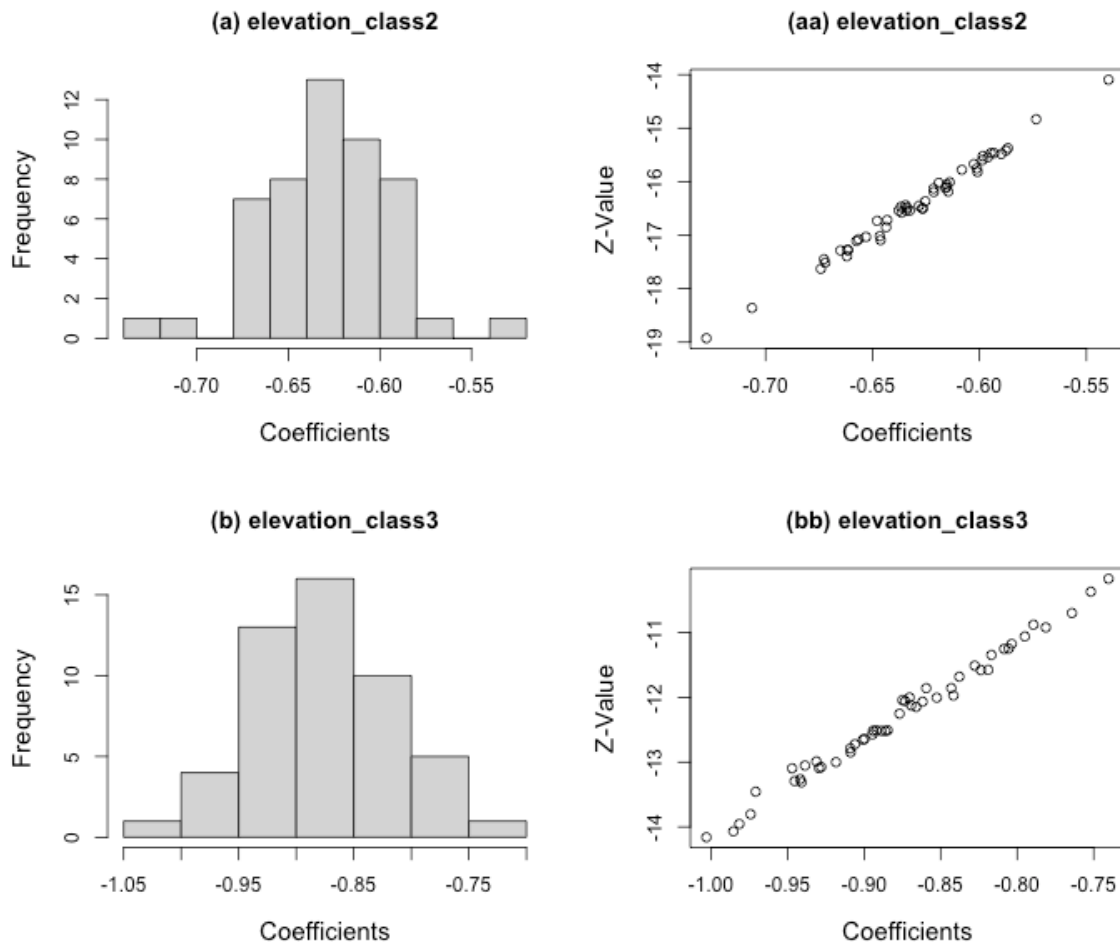
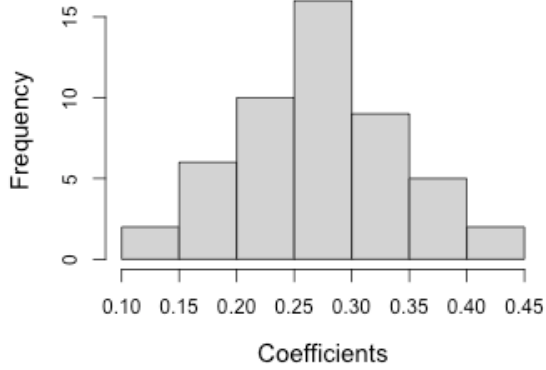


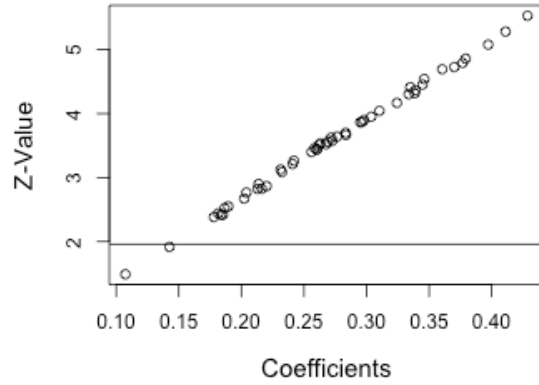
Figure S2. This figure shows the results of the sensitivity analysis found from 50 different logistic regression model runs for region wa2sf. Plots (a) – (v) are histograms of the coefficients. Plots (aa) – (vv) show the coefficients with their respective z-values plotted against them. In general, the coefficients for different variable classes are normally distributed and have consistent statistical significance (statistically significant if $|z\text{-values}| > 1.96$). Notable exceptions are the slope variables seen in plots (g) – (k). The coefficients with very different behavior have z-values near zero, indicating they were found to be highly insignificant predictors in their respective models.



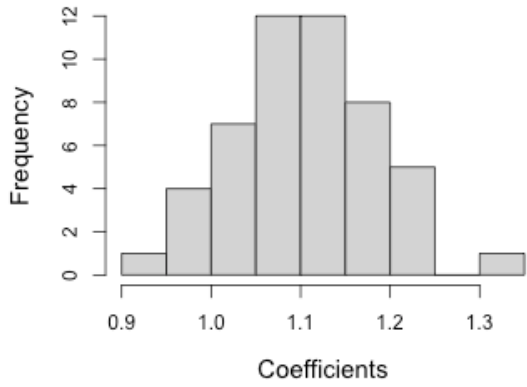
(c) elevation_class4



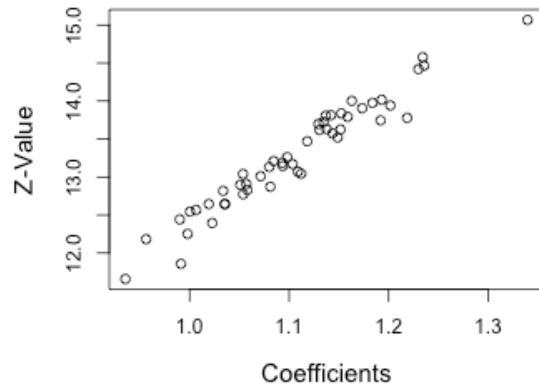
(cc) elevation_class4



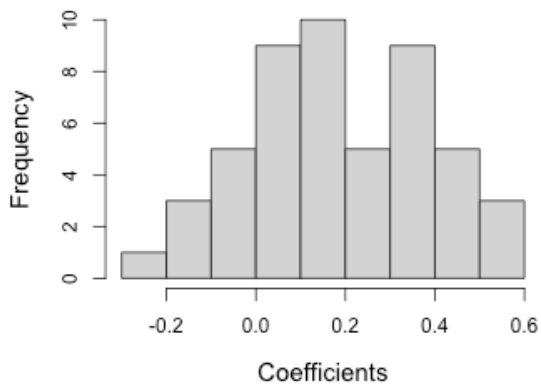
(d) elevation_class5



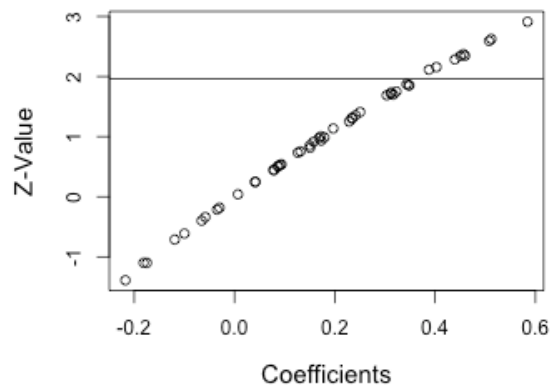
(dd) elevation_class5



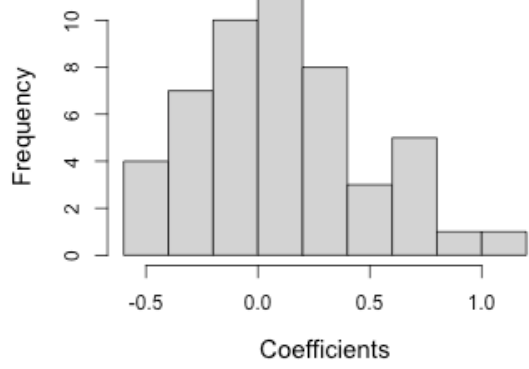
(e) elevation_class6



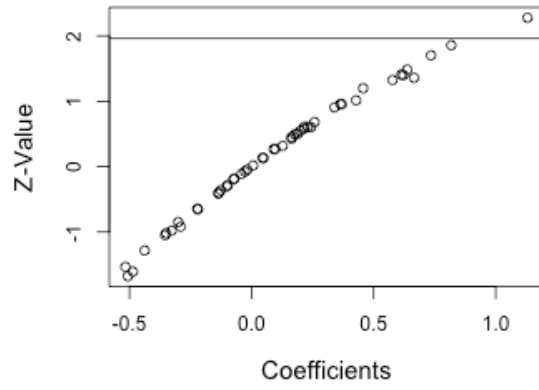
(ee) elevation_class6



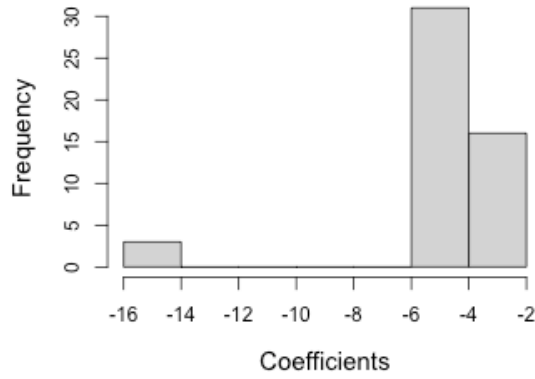
(f) elevation_class7



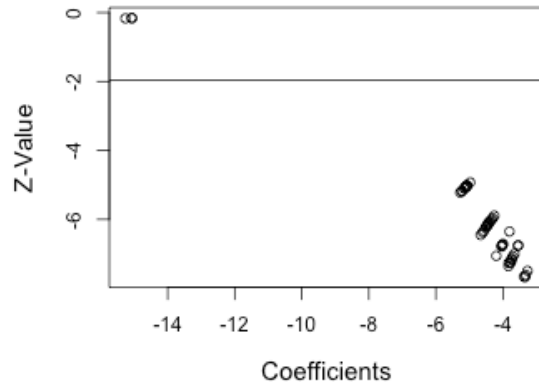
(ff) elevation_class7



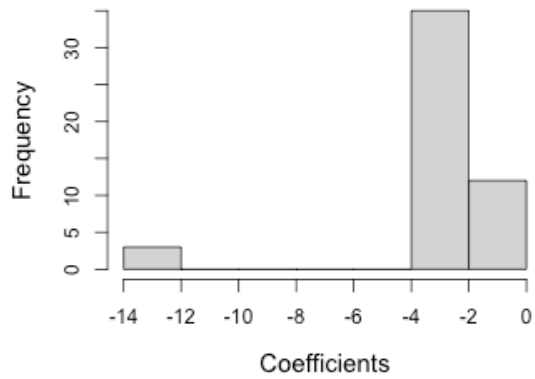
(g) slope_class0-10 deg



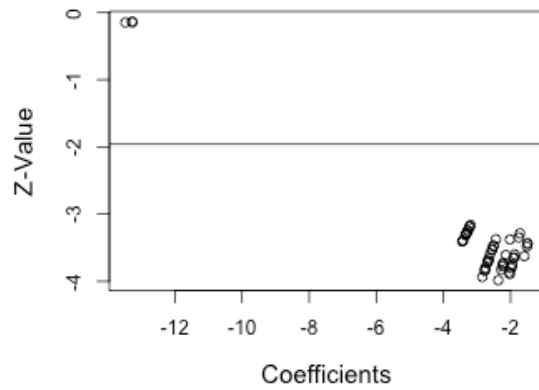
(gg) slope_class0-10 deg



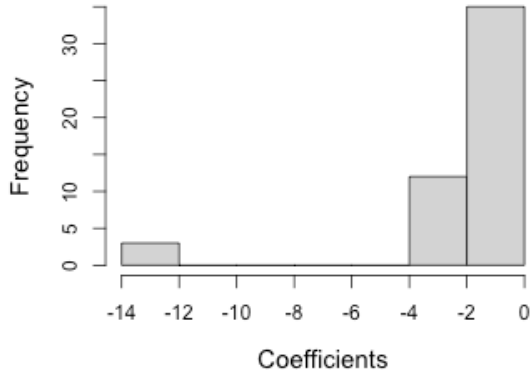
(h) slope_class10-20 deg



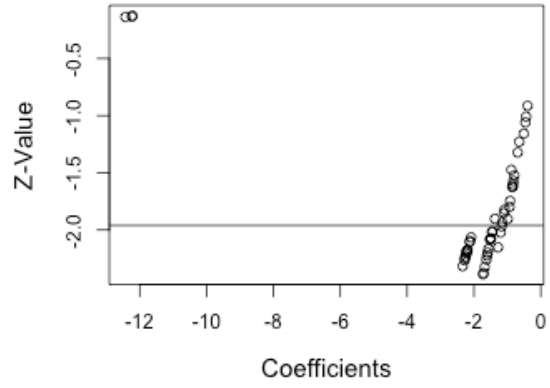
(hh) slope_class10-20 deg



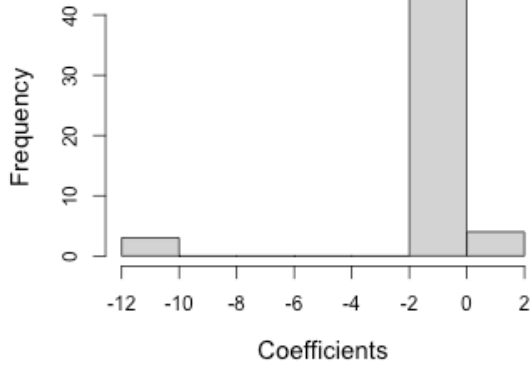
(i) slope_class20-30 deg



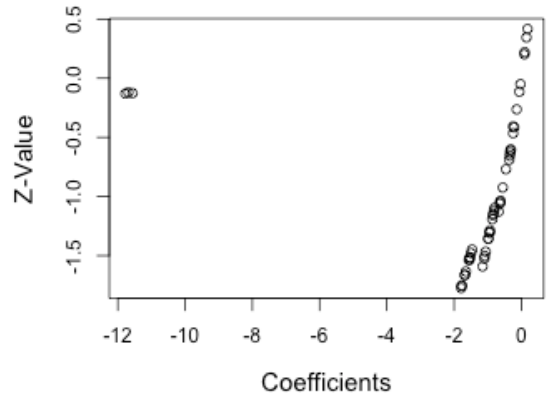
(ii) slope_class20-30 deg



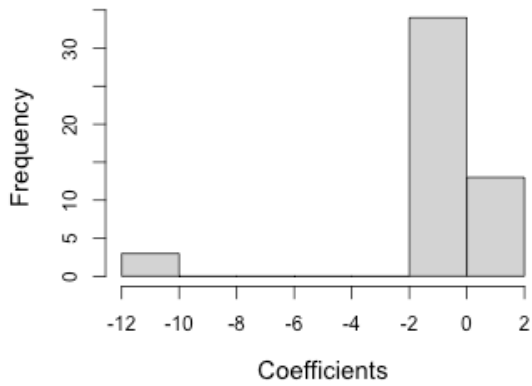
(j) slope_class30-40 deg



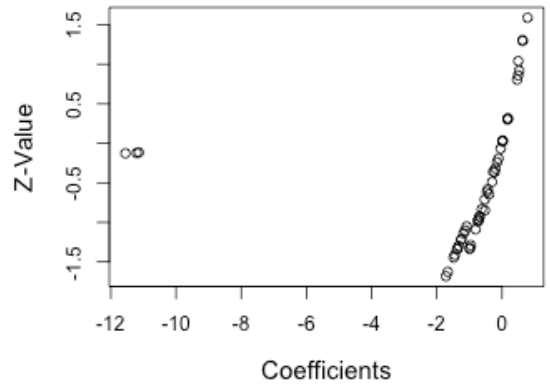
(jj) slope_class30-40 deg



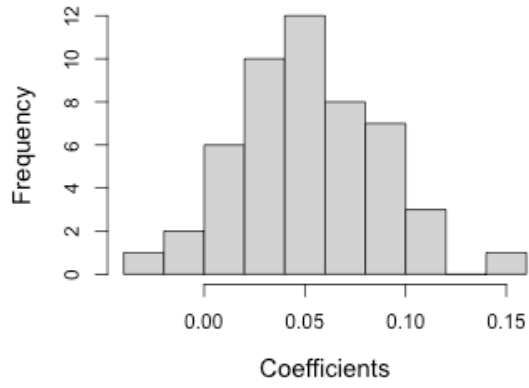
(k) slope_class40-50 deg



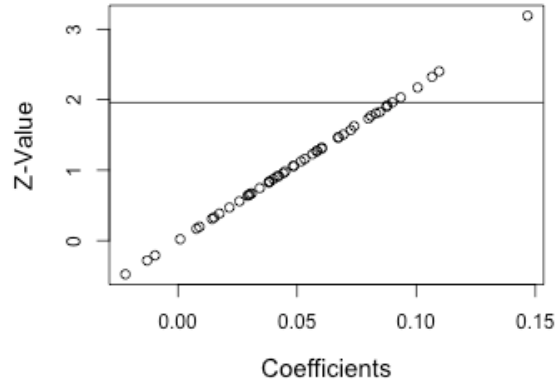
(kk) slope_class40-50 deg



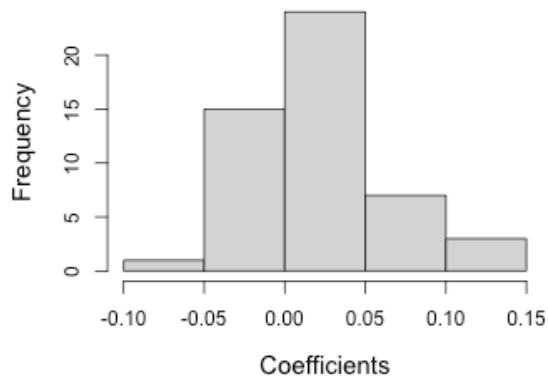
(l) aspect_classN



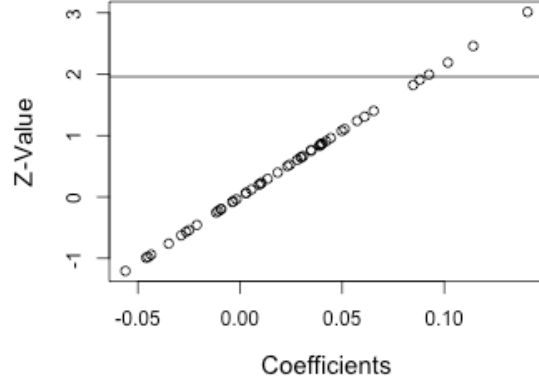
(ll) aspect_classN



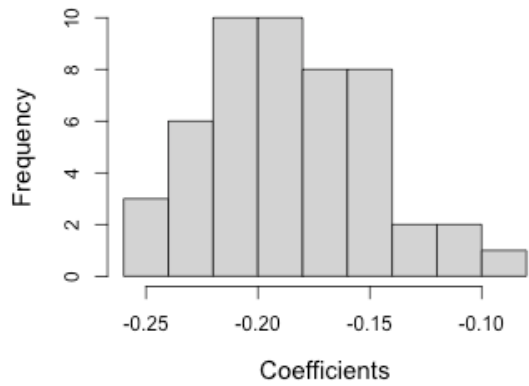
(m) aspect_classS



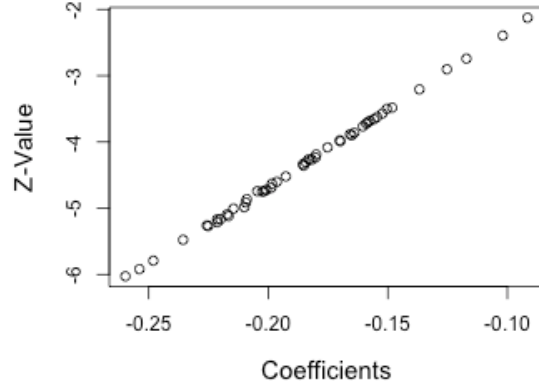
(mm) aspect_classS

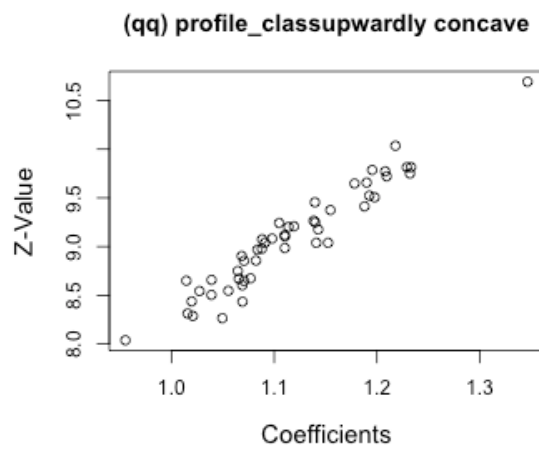
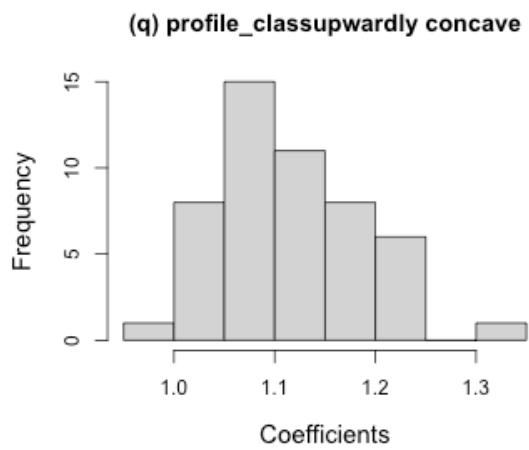
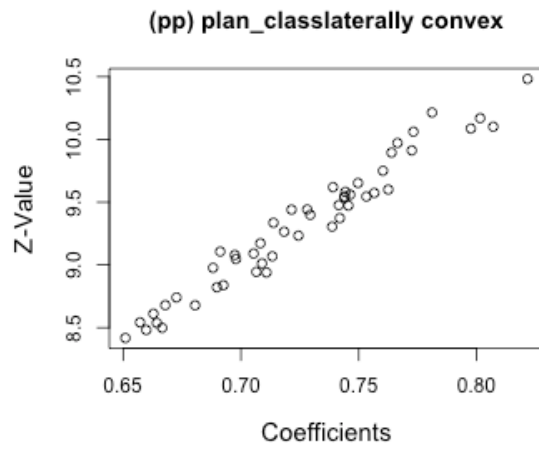
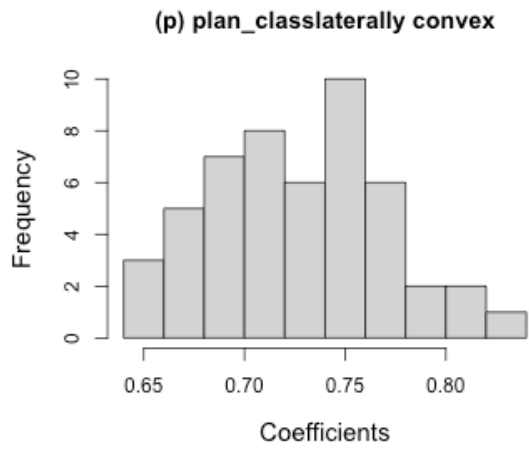
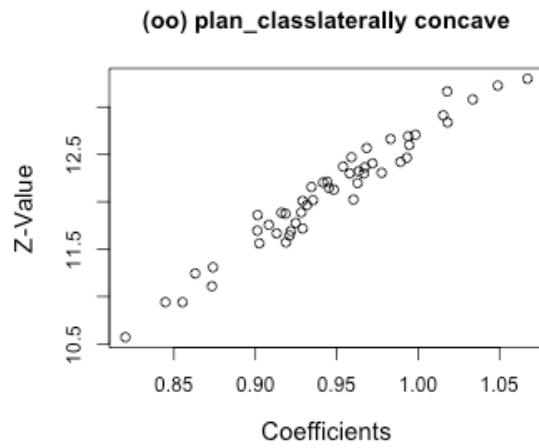
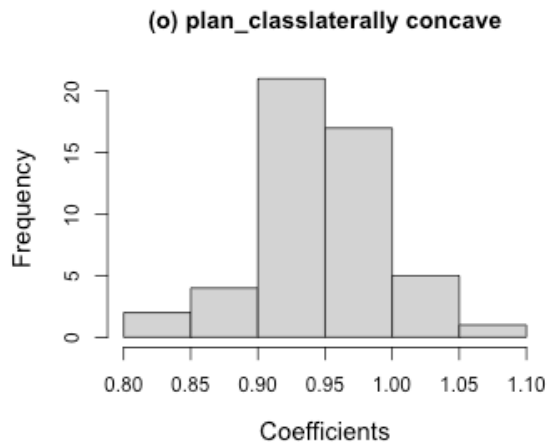


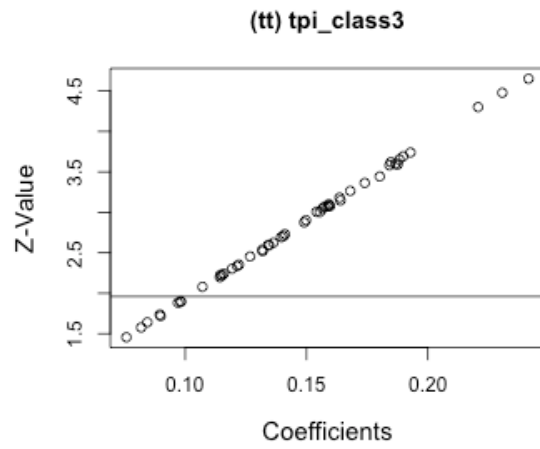
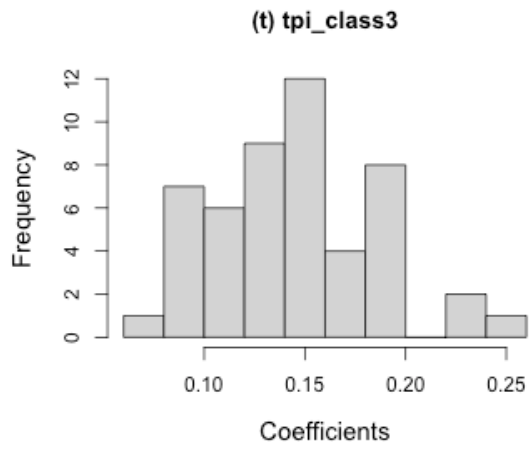
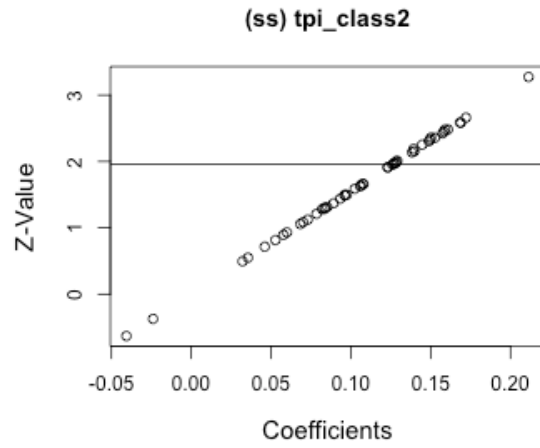
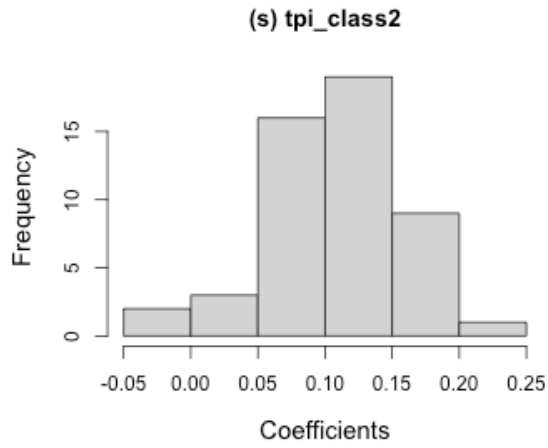
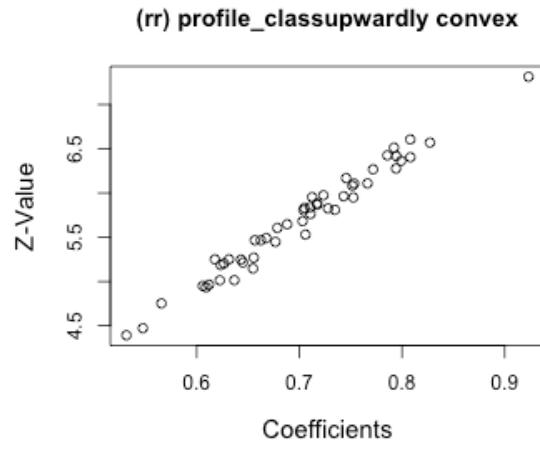
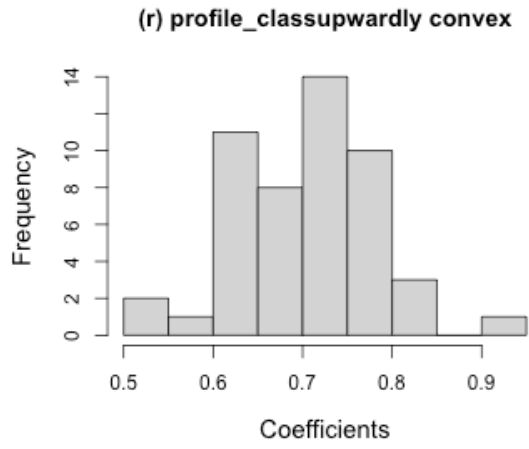
(n) aspect_classW

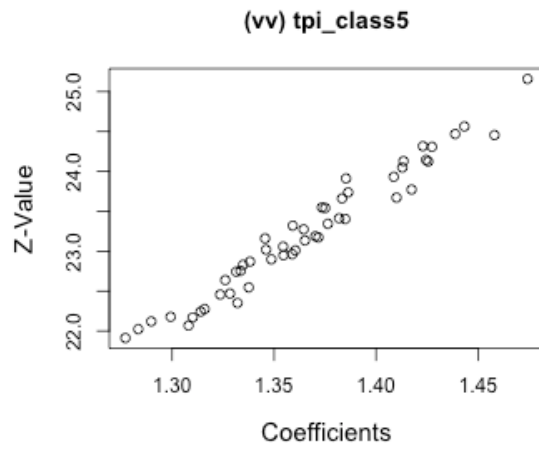
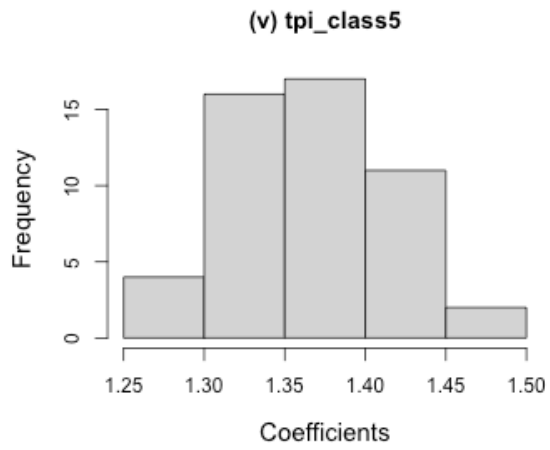
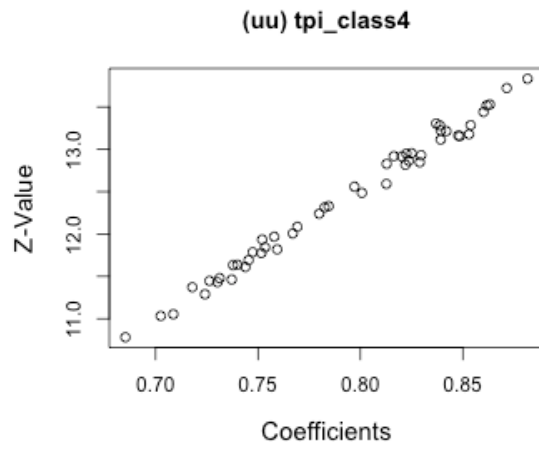
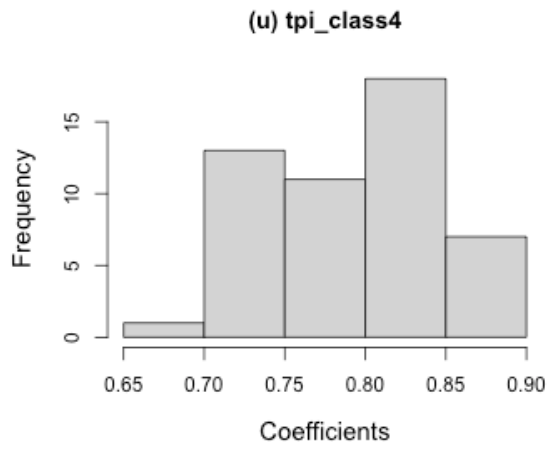


(nn) aspect_classW









Appendix A: Source Code

Source code is also available at <https://github.com/gmbelair1/landslide-susceptibility.git>

All code is written in R

Code:

```
#!/usr/bin/env Rscript

library(raster)
library(rpart)
library(pROC)

data_prep <- function(path){
  # Import Data
  # =====
  elevation = raster(file.path(path,"elevation.tif"))
  slope = raster(file.path(path,"slope.tif"))
  aspect = raster(file.path(path,"aspect.tif"))
  plan = raster(file.path(path,"plan.tif"))
  profile = raster(file.path(path,"profile.tif"))
  tpi = raster(file.path(path,"tpi.tif"))
  landslides = raster(file.path(path,"landslides.tif"))
  # Transform Data
  # =====
  datarast = stack(elevation,slope,aspect,plan,profile,tpi,landslides) # Stack raster datasets
  data = as.data.frame(datarast, xy = TRUE) # Coerce rasterstack into dataframe
  data$landslides[is.na(data$landslides)] = 0 # Set all landslide NA values to zero (so that
#ls isn't limiting factor)
  data = na.omit(data) # Omit any rows with NA values
  data = classify(data)
  data
}

# =====
# =====

classify = function(data){
  attach(data)
  # elevation
  if(exists("elevation")){
    erange = range(data$elevation, na.rm = T)
    brk = seq(erange[1]-1,erange[2]+1,length.out = 8)
    cls = as.character(1:7)
    elevation_class = cut(data$elevation, breaks = brk, labels = cls)
    elevation_class = as.character(elevation_class)
    data$elevation_class = elevation_class
  }
}
```

```

} else {data$elevation_class = NA}
# slope
if(exists("slope")){
  brk=c(-1,10,20,30,40,50,90)
  cls = c("0-10 deg","10-20 deg","20-30 deg","30-40 deg","40-50 deg", ">50 deg")
  slope_class = cut(data$slope, breaks = brk, labels = cls)
  slope_class = as.character(slope_class)
  data$slope_class = slope_class
} else {data$slope_class = NA}
# aspect
if(exists("aspect")){
  brk=c(-1,45,135,225,315,360)
  cls = c("N","E","S","W","N")
  aspect_class = cut(data$aspect, breaks = brk, labels = cls)
  aspect_class = as.character(aspect_class)
  data$aspect_class = aspect_class
} else {data$aspect_class = NA}
# plan
if(exists("plan")){
  plan_sd = sd(data$plan, na.rm = T)
  brk = c(min(data$plan, na.rm = T), -0.01, 0.01, max(data$plan, na.rm = T))
  cls = c("laterally concave", "flat", "laterally convex")
  plan_class = cut(data$plan, breaks = brk, labels = cls)
  plan_class = as.character(plan_class)
  data$plan_class = plan_class
} else {data$plan_class = NA}
# profile
if(exists("profile")){
  profile_sd = sd(data$profile, na.rm = T)
  brk = c(min(data$profile, na.rm = T), -0.01, 0.01, max(data$profile, na.rm = T))
  cls = c("upwardly concave", "flat", "upwardly convex")
  profile_class = cut(data$profile, breaks = brk, labels = cls)
  profile_class = as.character(profile_class)
  data$profile_class = profile_class
} else {data$profile_class = NA}
# tpi
if(exists("tpi")){
  tpi_sd = sd(data$tpi, na.rm = T)
  brk = c(min(data$tpi, na.rm = T), -tpi_sd, -0.5*tpi_sd, 0.5*tpi_sd, tpi_sd, max(data$tpi, na.rm =
T))
  cls = 1:5
  tpi_class = cut(data$tpi, breaks = brk, labels = cls)
  tpi_class = as.character(tpi_class)
  data$tpi_class = tpi_class
} else {data$tpi_class = NA}
data

```

```

}

# =====
# =====

ls_sample <- function(lpdata){
  # Input variables:
  # lpdata - data frame with binary landslide variable
  # p      - training percentage
  # index  - list that returns the indices of training and testing data
  ltrue = which(lpdata == 1)          # Indices of ls pixels
  xtrue <- sample(ltrue,length(ltrue), replace=F)    # Generate ls random nums from
#indices
  xtrue_train = xtrue[seq(1,p*length(ltrue))]      # p% of ls random nums
  xtrue_test  = xtrue[seq(p*length(ltrue),length(ltrue))]  # (1-p)% of ls random nums
  lsfalse = c(which(lpdata == 0), which(is.na(lpdata)))    # Indices of nonls pixels
  xfalse <- sample(lsfalse,length(ltrue), replace=F)      # Generate nonls random nums. Use
#length(ltrue) so there will be same num of nonls
  xfalse_train = xfalse[seq(1,p*length(ltrue))]          # p% of nonls random nums
  xfalse_test  = xfalse[seq(p*length(ltrue),length(ltrue))]  # (1-p)% of nonls random nums
  ind_train = c(xtrue_train, xfalse_train)
  ind_test  = c(xtrue_test, xfalse_test)
  index = list(train = ind_train, test = ind_test)
  index
}

# =====
# =====

fr_tabs <- function(data){
  # data$shaz = rep(0,length(data$x))
  attach(data)
  frtab = function(tab){
    ni = tab[,2]
    ai = tab[,1] + tab[,2]
    nr = sum(ni)
    ar = sum(ai)
    fr = (ni/ai)/(nr/ar)
    fr[is.nan(fr)] = 0
    fr
  }
  tabs = list(tab_elevation = 0, tab_slope = 0, tab_aspect = 0, tab_plan = 0, tab_profile = 0, tab_tpi
= 0)
  # Elevation
  if(!is.na(tabs$tab_elevation)){
    # Calculate FR
    cls = unique(data$elevation_class)
    tab = table(factor(data$elevation_class,cls),data$landslides)
  }
}

```

```

    tab_elevation = frtab(tab)
    tabs$tab_elevation = tab_elevation
  } else { tabs$tab_elevation = NA }
  # Slope
  if(!is.na(tabs$tab_slope)){
    # Calculate FR
    cls = unique(data$slope_class)
    tab = table(factor(data$slope_class,cls),data$landslides)
    tab_slope = frtab(tab)
    tabs$tab_slope = tab_slope
  }
  # Aspect
  if(!is.na(tabs$tab_aspect)){
    # Calculate FR
    cls = c("N","E","S","W")
    tab = table(factor(data$aspect_class,cls),data$landslides)
    tab_aspect = frtab(tab)
    tabs$tab_aspect = tab_aspect
  }
  # plan
  if(!is.na(tabs$tab_plan)){
    # Calculate FR
    cls = unique(data$plan_class)
    tab = table(factor(data$plan_class,cls),data$landslides)
    tab_plan = frtab(tab)
    tabs$tab_plan = tab_plan
  }
  # profile
  if(!is.na(tabs$tab_profile)){
    # Calculate FR
    cls = unique(data$profile_class)
    tab = table(factor(data$profile_class,cls),data$landslides)
    tab_profile = frtab(tab)
    tabs$tab_profile = tab_profile
  }
  # Classify the tpi
  if(!is.na(tabs$tab_tpi)){
    # Calculate FR
    cls = unique(data$tpi_class)
    tab = table(factor(data$tpi_class,cls),data$landslides)
    tab_tpi = frtab(tab)
    tabs$tab_tpi = tab_tpi
  }
  tabs
}

```

```

# =====
# =====
freq_ratio <- function(data, tabs){
  data$lshaz = rep(0,length(data$x))
  data$fr_elevation = tabs$tab_elevation[data$elevation_class]
  data$lshaz = data$lshaz + data$fr_elevation
  data$fr_slope = tabs$tab_slope[data$slope_class]
  data$lshaz = data$lshaz + data$fr_slope
  data$fr_aspect = tabs$tab_aspect[data$aspect_class]
  data$lshaz = data$lshaz + data$fr_aspect
  data$fr_plan = tabs$tab_plan[data$plan_class]
  data$lshaz = data$lshaz + data$fr_plan
  data$fr_profile = tabs$tab_profile[data$profile_class]
  data$lshaz = data$lshaz + data$fr_profile
  data$fr_tpi = tabs$tab_tpi[data$tpi_class]
  data$lshaz = data$lshaz + data$fr_tpi
  data[is.na(data)] = 0
  data$lshaznorm = (data$lshaz - min(data$lshaz))/(max(data$lshaz)-min(data$lshaz))
  data
}

# =====
# =====
haz_results <- function(data, p, path = NULL){
  # Hazard code specifically for the cluster
  # data: classified data layer. Should contain 13 vars: x, y, elevation, slope, aspect
  #   plan, profile, tpi, landslides, elevation_class, slope_class, aspect_class,
  #   plan_class,profile_class, tpi_class
  # p : decimal percent used for training
  # path: path where you want the results saved
  library(rpart)
  library(pROC)
  #if(!dir.exists(path)){dir.create(path)} # create folder for results if it doesn't already exist

  # Determine training and testing data
  i = ls_sample(data$landslides,p) # p/(1-p) Indices
  print(length(i$train))
  e = unique(data$elevation_class); s = unique(data$slope_class); a = unique(data$aspect_class);
  pr = unique(data$profile_class); pl = unique(data$plan_class); t = unique(data$tpi_class)
  i2 = c()
  for(n in 1:length(e)){i2 = append(i2, which(data$elevation_class == e[n])[1])}
  for(n in 1:length(s)){i2 = append(i2, which(data$slope_class == s[n])[1])}
  for(n in 1:length(a)){i2 = append(i2, which(data$aspect_class == a[n])[1])}
  for(n in 1:length(pr)){i2 = append(i2, which(data$profile_class == pr[n])[1])}
  for(n in 1:length(pl)){i2 = append(i2, which(data$plan_class == pl[n])[1])}
  for(n in 1:length(t)){i2 = append(i2, which(data$tpi_class == t[n])[1])}

```

```

i2 = na.exclude(i2)
i$train = append(i$train, i2)
print(length(i$train))

dataP = data[i$train,]          # Training data, p% of data
dataP = na.omit(dataP)
dataQ = data[i$test,]         # Testing data, (1-p)% of data
dataQ = na.omit(dataQ)
#saveRDS(data, file = file.path(path,"data.rds"))
#saveRDS(i$train, file = file.path(path,"train.rds"))
#saveRDS(i$test, file = file.path(path,"test.rds"))

lrP = glm(landslides ~
elevation_class+slope_class+aspect_class+plan_class+profile_class+tpi_class,data=dataP,
family=binomial)
print(summary(lrP))
lrProc = roc(dataP$landslides, lrP$fitted.values)    # Validation ROC
print(lrProc)
lrQ = predict(lrP, dataQ, type = "response")        # 30% data prediction values
lrQroc = roc(dataQ$landslides, lrQ)                 # 30% data prediction ROC
print(lrQroc)
lr = list(lrP = lrP, lrProc = lrProc, lrQ = lrQ, lrQroc = lrQroc)
#saveRDS(lr, file = file.path(path,"lr.rds"))

# Frequency Ratio
tabs = fr_tabs(dataP)
print(tabs)
frP = freq_ratio(dataP, tabs)
print(summary(dataP))
print(summary(frP$shaznorm))
frProc = roc(dataP$landslides, frP$shaznorm)        # Validation ROC
print(frProc)
frQ = freq_ratio(dataQ, tabs)                       # Prediction values
frQroc = roc(dataQ$landslides, frQ$shaznorm)        # Prediction ROC
print(frQroc)
fr = list(tabs = tabs,frProc = frProc, frQroc = frQroc)
#saveRDS(fr, file = file.path(path,"fr.rds"))

# Logistic Regression
lrdf = as.data.frame(summary(lrP)$coefficients)
#write.csv(lrdf, file.path(path, "lr.csv"))

# Frequency Ratio
elevationdf = as.data.frame(tabs$tab_elevation)
elevationdf$var = rep("elevation",length(elevationdf))
colnames(elevationdf) = c("LSI", "var")

```

```

slopedf = as.data.frame(tabs$tab_slope)
slopedf$var = rep("slope",length(slopedf))
colnames(slopedf) = c("LSI", "var")
aspectdf = as.data.frame(tabs$tab_aspect)
aspectdf$var = rep("aspect",length(aspectdf))
colnames(aspectdf) = c("LSI", "var")
plandf = as.data.frame(tabs$tab_plan)
plandf$var = rep("plan",length(plandf))
colnames(plandf) = c("LSI", "var")
profiledf = as.data.frame(tabs$tab_profile)
profiledf$var = rep("profile",length(profiledf))
colnames(profiledf) = c("LSI", "var")
tpidf = as.data.frame(tabs$tab_tpi)
tpidf$var = rep("tpi",length(tpidf))
colnames(tpidf) = c("LSI", "var")
frdf = rbind(elevationdf, slopedf, aspectdf, plandf, profiledf, tpidf)
#write.csv(frdf, file = file.path(path,"fr.csv"))

lr_fr = list(lrP = lrP, lrProc = lrProc, lrQ = lrQ, lrQroc = lrQroc, tabs = tabs, frProc = frProc,
frQroc = frQroc)
lr_fr
}

data_prep_mix <- function(path1, path2){
# Import Data for region 1
elevation1 = raster(file.path(path1,"elevation.tif"))
slope1 = raster(file.path(path1,"slope.tif"))
aspect1 = raster(file.path(path1,"aspect.tif"))
plan1 = raster(file.path(path1,"plan.tif"))
profile1 = raster(file.path(path1,"profile.tif"))
tpi1 = raster(file.path(path1,"tpi.tif"))
landslides1 = raster(file.path(path1,"landslides.tif"))
# Transform Data for region 1
datarast1 = stack(elevation1,slope1,aspect1,plan1,profile1,tpi1,landslides1) # Stack raster
datasets
data1 = as.data.frame(datarast1, xy = TRUE) # Coerce rasterstack into
dataframe
data1$landslides[is.na(data1$landslides)] = 0 # Set all landslide NA values to zero (so
that ls isn't limiting factor)
data1 = na.omit(data1) # Omit any rows with NA values

# Import Data for region 2
elevation2 = raster(file.path(path2,"elevation.tif"))
slope2 = raster(file.path(path2,"slope.tif"))
aspect2 = raster(file.path(path2,"aspect.tif"))
plan2 = raster(file.path(path2,"plan.tif"))

```

```

profile2 = raster(file.path(path2,"profile.tif"))
tpi2 = raster(file.path(path2,"tpi.tif"))
landslides2 = raster(file.path(path2,"landslides.tif"))
# Transform Data for region 2
datarast2 = stack(elevation2,slope2,aspect2,plan2,profile2,tpi2,landslides2) # Stack raster
datasets
data2 = as.data.frame(datarast2, xy = TRUE) # Coerce rasterstack into
dataframe
data2$landslides[is.na(data2$landslides)] = 0 # Set all landslide NA values to zero (so
that ls isn't limiting factor)
data2 = na.omit(data2) # Omit any rows with NA values

data12 = rbind(data1,data2)
data_mix = classify(data12)

data1_class = classify(data1)
data2_class = classify(data2)
data_sep = rbind(data1_class, data2_class)

data = list(data_mix = data_mix, data_sep = data_sep)
}

```